Hybrid Encapsulated Ionic Liquids for Post-Combustion Carbon Dioxide (CO_2) Capture

Budget Period 1 - Topical Report

Reporting Period:	October 1, 2015 to September 30, 2016
Project Period:	October 1, 2015 to September 30, 2018
Principal Authors:	Joan F. Brennecke*+, Thomas F. Degnan*, Mark J. McCready*, Mark A. Stadtherr*, Joshuah K. Stolaroff**, and Congwang Ye**
	*University of Notre Dame, Department of Chemical and Biomolecular Engineering **Lawrence Livermore National Laboratory +Principal Investigator
Date Report Issued:	November 2016
DOE Award Number:	DE-FE0026465
Submitting Organization/: Recipient	University of Notre Dame du lac Office of Research 940 Grace Hall Notre Dame, IN 46556
Prepared for:	United States Department of Energy Office of Fossil Energy National Energy Technology Laboratory

DISCLAIMER

ABSTRACT

Ionic liquids (ILs) and Phase Change Ionic Liquids (PCILs) are excellent materials for selective removal of carbon dioxide from dilute post-combustion streams. However, they are typically characterized as having high viscosities, which impairs their effectiveness due to mass transfer limitations, caused by the high viscosities. In this project, we are examining the benefits of encapsulating ILs and PCILs in thin polymeric shells to produce particles of approximately 100 to 600 μm in diameter that can be used in a fluidized bed absorber. The particles are produced by microencapsulation of the ILs and PCILs in CO_2-permeable polymer shells. Here we report on the synthesis of the IL and PCIL materials, measurements of thermophysical properties including CO_2 capacity and reprotonation equilibrium and kinetics, encapsulation of the ILs and PCILs, mechanical and thermodynamic testing of the encapsulated materials, development of a rate based model of the absorber, and the design of a laboratory scale unit to test the encapsulated particles for CO_2 capture ability and efficiency. We show that the IL/PCIL materials can be successfully encapsulated, that they retain CO_2 uptake capacity, and that the uptake rates are increased relative to a stagnant sample of IL liquid or PCIL powder.

TABLE OF CONTENTS

INTRODUCTION

The principal objective of this project is to demonstrate (TRL 3-4) the use of hybrid encapsulated ionic liquids (ILs) or phase change ionic liquids (PCILs) for post-combustion CO_2 capture. Encapsulated ILs/PCILs typically have high surface areas, allowing us to traverse the mass transfer barriers caused by high viscosities that are characteristic of ILs and PCILs.

This topical report describes work completed in Budget Period 1 of this project. The objectives for Budget Period 1 were to show that ILs and/or PCILs can be encapsulated, that they retain high CO_2 capture efficiency and recyclability, and that their use in a fluidized and/or packed bed is feasible.

RESULTS AND DISCUSSION

Budget Period 1 was comprised of a single task for project management and five technical tasks related to synthesis, encapsulation, and testing of ILs and PCILs; development of a rate-based model to establish targets for necessary improvements in mass transfer; and the design of a laboratory-scale test unit. The following describes work completed for the five technical tasks.

Task 2.0 – Synthesis and Testing of IL and PCIL Candidates

Subtask 2.1 - Synthesis and purification

In the first year of this project, we successfully synthesized and tested nine IL and ten PCIL candidate materials – see **Tables 1, 2** and **4** below. These ILs and PCILs were synthesized using standard alkylation and ion exchange methods. The purity of the ILs and PCILs was ascertained by ^{1}H NMR spectroscopy. These specific ILs and PCILs were chosen based on our prior extensive experience with these types of materials. We have previously shown that the enthalpy of reaction with CO_2 needs to be between about -45 and -60 kJ/mole to minimize the energy requirements for the CO_2 capture process **[1]**. We chose anions that, based on prior experience and previous density functional theory (DFT) calculations, should be in this range **[2].**

ILs need to be liquid at absorption conditions (e.g., 40 °C) and the viscosity needs to be as low as possible to eliminate mass transfer resistances within the capsules. We have previously shown that this can be achieved by shortening alkyl chain lengths somewhat and incorporating ether groups **[3, 4]**. PCILs must have higher melting points for the pure materials, but the melting point needs to decrease when the PCIL reacts with CO_2. In an earlier project we were not able to develop a theoretical model that could accurately predict this property. Therefore, the selection of PCIL candidates for this project was guided primarily by previous experience **[5]**.

All of the thermophysical properties needed to perform an initial evaluation of an IL or PCIL (see Subtasks 2.2 and 2.3, below) can be conducted in our laboratories using just 5 g of IL or PCIL. We synthesized 10 and 20 g batches of four ILs and PCILs for compatibility testing and encapsulation by our project partner, Lawrence Livermore National Laboratory (LLNL). These were NDIL230, NDIL0231, NDIL0252 and NDIL0274. Additional larger batches of the top IL candidate (NDIL0230), totaling 240 g, were synthesized and provided to LLNL. Sufficient quantities of the PCIL NDIL0309 were already on hand, and more than 100 g have been supplied to LLNL.

The LLNL apparatus is sized for a minimum of 2 to 3 g of encapsulated liquid to allow for 'line-out' and production of representative samples of encapsulated capsules. As described below, LLNL has performed many different encapsulation runs with NDIL0230 and NDIL0309 in their work to optimize encapsulation conditions. Sufficient quantities of representative capsules were required for CO_2 uptake measurements and NMR analysis at Notre Dame. Even larger quantities of capsules of the preferred IL and PCIL, NDIL0230 and NDIL0309, are needed to meet the material requirements for the Laboratory Scale Unit (see below). A key criterion in the design of the Laboratory Scale Unit (LSU) was to use a minimum amount of encapsulated IL or PCIL to accurately simulate the CO_2 uptake and regeneration of encapsulated ILs and PCILs in a fluidized bed.

Table 1 below provides a list of the ILs that were synthesized for this project and sent to LLNL for encapsulation. In addition, six more batches of NDIL0230 were synthesized for use by researchers at Notre Dame. Finally, more than 100 g of NDIL0309, which was synthesized prior to the start of this project, was sent to LLNL for encapsulation.

Table 1: List of IL samples that were synthesized for this project and sent to LLNL for encapsulation.

IL Sample	Amount	Date sent to LLNL
NDIL0230	10 g	Aug 28 2015
NDIL0231	10 g	Aug 28 2015
NDIL0252	10 g	Aug 28 2015
NDIL0274	10 g	Aug 28 2015
NDIL0230	20 g	Oct 9 2015
NDIL0231	20 g	Oct 9 2015
NDIL0252	20 g	Oct 9 2015
NDIL0274	20 g	Oct 9 2015
NDIL0230	50 g	Feb 15 2016
NDIL0230	45 g	May 11 2016
NDIL0230	145 g	Aug 2 2016

Subtask 2.2 - Physical property characterization

In order to evaluate the suitability of the candidate materials, we measured the melting points, decomposition temperatures, densities, and viscosities of all IL and PCIL materials synthesized in this project for which these measurements were possible. We also measured the enthalpy of fusion of the following materials: NDIL0309, NDIL0312, NDIL0315, NDIL0317, NDIL0319, NDIL0320, and NDIL0335. The melting point and/or glass transition temperature and decomposition temperature are measured for each batch of every IL or PCIL sample synthesized, which provides an assessment of purity that complements the ^{1}H NMR analysis.

The melting point (T_m), glass transition temperature (T_g), and enthalpy of fusion were measured with a model DSC 822 Mettler-Toledo differential scanning calorimeter (DSC), which is equipped with the Mettler-Toledo STAR^e software version 9.10. The samples are run in aluminum crucibles (Mettler Toledo Al-Crucibles standard 40 μL) with nitrogen (Airgas, high purity, Grade 4.8) as the purging gas at 50 ml/min. 10-20 mg of sample was used. For samples that are liquid at room temperature, thermograms were recorded from 153 K to 323 K after cooling from 298 K to 153 K. For samples that were solid at room temperature, thermograms were recorded from 153 K to 383 K, after cooling from 383 K to 153 K. Both heating and cooling rates were 10 K/min. The melting point (T_m) was determined to be the onset temperature of an endothermic peak upon heating, and the glass transition temperature (T_g) was determined as the temperature at the midpoint of a small heat capacity change. The uncertainties of T_m and T_g are ± 2 K.

The decomposition temperatures were measured with a Mettler-Toledo TGA/SDTA 851e/SF/1100^{o}C thermal gravimetric analyzer, using the same software as above. All samples were run in aluminum crucibles (Mettler Toledo Al-Crucibles standard 40 μL) with nitrogen (same as above) as the purging gas at 50 ml/min. 15-25 mg of sample was used. In a typical experiment, the sample was dried in situ at 383 K for 45 minutes, and then heated to 773 K at 10 K/min. Relative thermal stabilities were described by the onset temperatures (T_{onset}), which is defined as the measured sample temperature at the intersection of the baseline before decomposition and the step tangent of weight vs. time curve as decomposition occurs. The largest uncertainty is from manually determining the tangent point for the onset temperature, which results in an uncertainty in the onset temperature of ±2 K.

The density of each IL was measured with an oscillating u-tube Anton Paar 4500 densitometer. The instrument requires approximately 1.7 mL of sample and reportedly has ± 0.00005 g cm^{-3} uncertainty. However, when taking the sample impurities into account, we estimate the uncertainty in the density measurements to be ± 0.002 g cm^{-3}. The density was normally measured from 283.15 K to 353.15 K, in 5 K to 10 K increments. This instrument can only measure the density of liquids; therefore, the densities of the solid PCIL candidates are not measured.

The viscosity of each IL, which was liquid at room temperature and did not have excessively high viscosity, was measured with a cone and plate ATS Viscoanalyzer under

a flow of dry nitrogen to prevent absorption of water from the atmosphere. The instrument requires 0.3-0.4 mL of sample and the estimated uncertainty is ±6%. The viscosity was normally measured between 278.15 K and 343.15 K, in 5 K or 10 K increments.

Table 2 below, summarizes the status of the measurements and the conclusions from the characterization of the 9 ILs synthesized for this project. The glass transition temperatures, melting temperatures, decomposition temperatures and viscosity and density at 40^{o}C for the IL candidates are shown in **Table 3**. The values shown are for a representative batch of each of the ILs. The values for all of the batches synthesized are consistent within the experimental uncertainties reported above.

Table 2: Measurements made and status of nine IL candidates considered for this project

Ionic Liquid Candidates

	Viscosity	Density	Melting Point	Decomposition Temperature	CO2 Solubility/ Uptake	Compatiblity with LLNL Shell Materials	Conclusion
NDIL0252	M	M	M	M	M	M	Not compatible with LLNL encapsulation materials
NDIL0274	M	M	M	M	M	M	Not compatible with LLNL encapsulation materials
NDIL0230	M	M	M	M	M	M	All properties look good; viable candidate for encapsulation
NDIL0231	M	M	M	M	M	M	MP of the IL increases when contacted with CO2 - full isotherms could not be measured over range of interest. Disqualified as a potential candidate
NDIL0303	NM	NM	NM	NM	NM	NM	IL decomposes; physical measurements unreliable; disqualified as a potential candidate
NDIL0304	NM	NM	NM	NM	NM	NM	IL decomposes; physical measurements unreliable; disqualified as a potential candidate
NDIL0313	NM	NM	NM	NM	NM	NM	IL decomposes; physical measurements unreliable; disqualified as a potential candidate
NDIL0316	M	M	M	M	M	NM	IL is too viscous; not a viable candidate
NDIL0336	M	M	M	M	M	M	All properties look good; viable candidate for encapsulation

Memo (In the above table):
M = Measured
NM = Not Measured

Table 3: Melting Points, Decomposition Temperatures, Densities and Viscosities at 40 °C of the IL candidates

Ionic Liquid	Density	Viscosity	T_g (K)	T_m (K)	T_{dec} (K)
NDIL0252	0.892	160	198		591
NDIL0274	0.910	170	197		570
NDIL0230	0.946	80	194		505
NDIL0231	0.978	190	208	266	556
NDIL0316*	1.147	482		221	579
NDIL0336*	0.983	263	216		536

*Densities and viscosities at 45 ^{O}C

Based on these analyses, two of the nine IL materials, which are highlighted in yellow, continue to look attractive as potential candidates for encapsulation.

Table 4 below, summarizes the status of the measurements and the conclusions from the characterization of the 10 PCILs synthesized for this project. Melting points and decomposition temperatures of the PCIL candidates are shown in **Table 5**.

Table 4: Measurements made and status of ten PCIL candidates considered for this project

Phase Change Ionic Liquid Candidates

	Viscosity	Density	Melting Point	Decomposition Temperature	CO2 Solubility/ Uptake	Compatiblity with LLNL Shell Materials	Conclusion
NDIL0309	M*	M*	M	M	M	M	All properties look good; viable candidate for encapsulation; *measured saturated with CO2 so that it is a liquid. Viscosity and density cannot be measured for solids
NDIL0312	NM	NM	NM	NM	NM	NM	PCIL decomposes; physical measurements unreliable; disqualified as a potential candidate
NDIL0314	NM	NM	NM	NM	NM	NM	PCIL decomposes; physical measurements unreliable; disqualified as a potential candidate
NDIL0315	NM	NM	NM	NM	NM	NM	PCIL decomposes; physical measurements unreliable; disqualified as a potential candidate
NDIL0317	NM	NM	M	M	M	NM	This compound does not show PCIL properties (i.e., the melting point of the complex with CO2 is not significantly lower than the melting point of the pure material). It has been disqualified as a candidate for encapsulation.
NDIL0319	NM	NM	NM	NM	NM	NM	PCIL decomposes; physical measurements unreliable; disqualified as a potential candidate
NDIL0320	NM	NM	M	M	M	NM	This compound does not show PCIL properties (i.e., the melting point of the complex with CO2 is not significantly lower than the melting point of the pure material). It has been disqualified as a candidate for encapsulation.
NDIL0335	NM	NM	M	M	M	M	This compound was originally intended to be an IL candidate but the melting point was higher than anticipated. Therefore, it has been designated as a PCIL candidate. All properties look good; viable candidate for encapsulation
NDIL0346	NM	NM	M	M	M	NM	This compound does not show PCIL properties (i.e., the melting point of the complex with CO2 is not significantly lower than the melting point of the pure material). It has been disqualified as a candidate for encapsulation.
NDIL0347	NM	NM	M	M	M	NM	This compound does not show PCIL properties (i.e., the melting point of the complex with CO2 is not significantly lower than the melting point of the pure material). It has been disqualified as a candidate for encapsulation.

Memo (In the above table):
M = Measured
NM = Not Measured

Table 5: Melting Points and Decomposition Temperatures of the PCIL Candidates

Ionic Liquid	$T_{Melting}$ (°C)	$T_{Decomposition}$ (°C)	Comments
NDIL0309	166	311(N_2) / 311 (air)[1]	Shows PCIL behavior
NDIL0312	98	260	Shows PCIL behavior, but appears to decompose so numbers may not be accurate
NDIL0317	86	285	Does not show PCIL behavior; turns solid again after stirring
NDIL0320	82	290	Does not show PCIL behavior; turns solid again after stirring
NDIL0335	66 / 103 (Two peaks)	312	Shows PCIL behavior
NDIL0346	44	288	Does not show PCIL behavior; remains solid after exposure to CO_2
NDIL0347	11 / 25 (Two peaks)	301	Does not show PCIL behavior; turns solid after exposure to CO_2

[1] Values from Reference [5]

Based on these analyses, two of the ten PCIL materials continue to look attractive as potential candidates for encapsulation.

Subtask 2.3 - CO_2 uptake measurements

We measured the CO_2 uptake for the following IL and PCIL candidates at the temperatures indicated: NDIL0230 (22 °C, 40 °C and 60 °C), NDIL0336 (60 °C), and NDIL0335 (40 °C). (The CO_2 uptake of NDIL0309 at 60 ºC, 70 ºC, and 80 ºC was measured as part of a previous project **[5])**. The uptake experiments are done either volumetrically or gravimetrically. The volumetric apparatus consists of a stirred sample cell containing about 1 g of IL, along with a calibrated delivery tank, both of which are located in a constant temperature oven. The CO_2 uptake is determined by the calculating the number of moles of CO_2 transferred into the liquid from the changes in pressure, using the ideal gas law. This apparatus is used from approximately 10 mbar to 1 bar pressure. The gravimetric method uses a Hiden Intelligent Gravimetric Analyzer. This system requires only 75 mg of sample and can go to 15 bar. However, the measurements for this project are only to 1 bar. Both systems yield consistent results to within +/- 0.02 mol CO_2/mol IL. We found that the uptake is quite high even at low CO_2 partial pressures, as is desired for post-combustion CO_2 capture. The CO_2 uptake data are shown in **Figures 1 to 4**. Note that the higher temperature data for NDIL0230 is still being analyzed. All four of these ILs appear to be viable candidates, although the strong uptake for NDIL0336 at 60 °C indicates that its enthalpy of reaction may be a bit too strong (i.e., it would require a bit more energy to reverse the reaction in the stripper). This is further supported by observation of very slow degradation as a function of time

during the uptake measurements (i.e., anions that react strongly with CO_2 also tend to be sufficiently basic that they can degrade the cation).

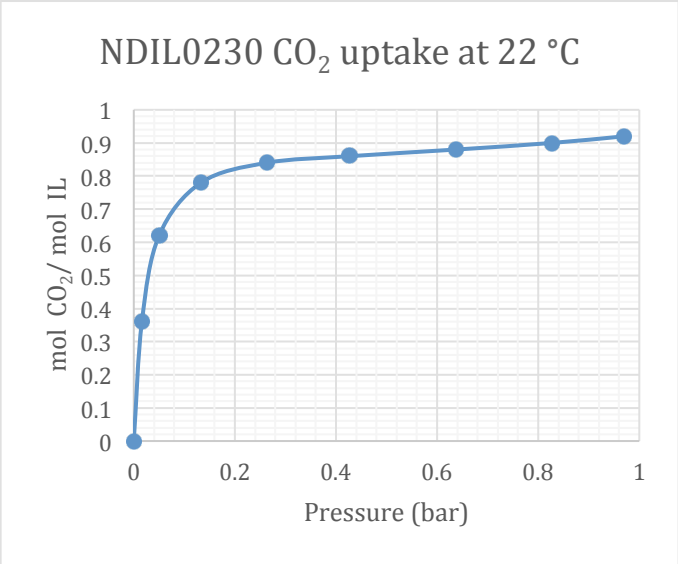

Figure 1: CO_2 uptake at 22 °C for NDIL0230

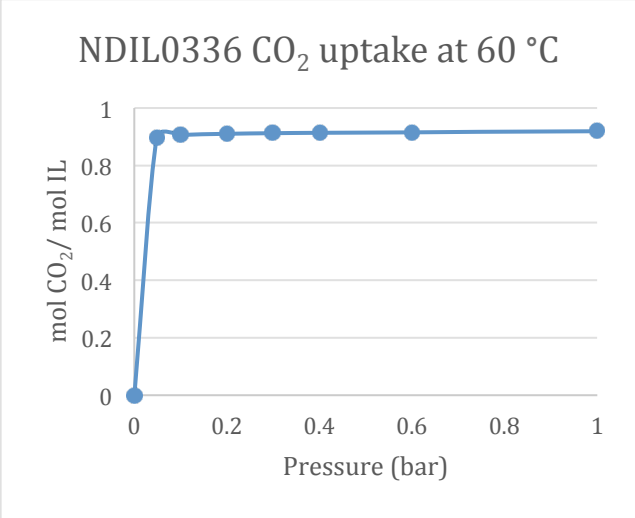

Figure 2: CO_2 uptake at 60 °C for NDIL0336

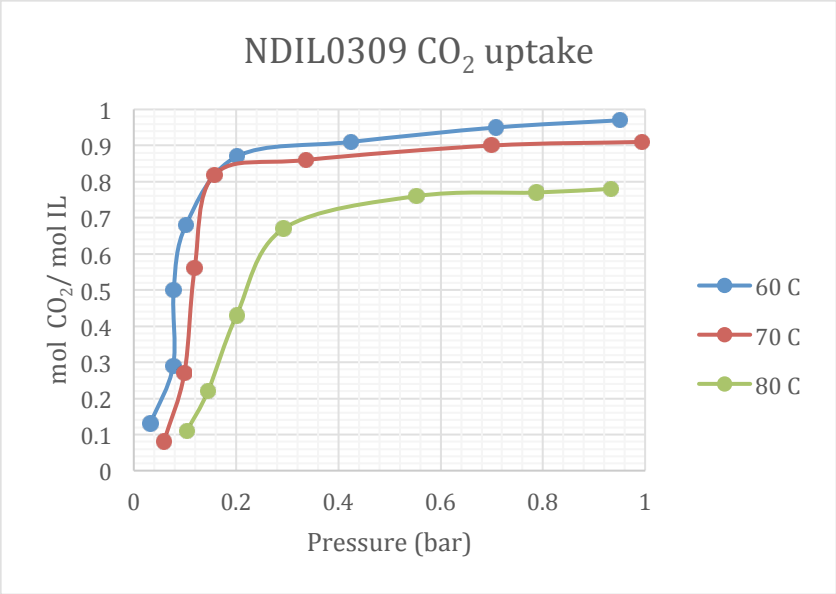

Figure 3: CO_2 uptake at 60, 70 and 80 °C for NDIL0309 (from Reference [5]).

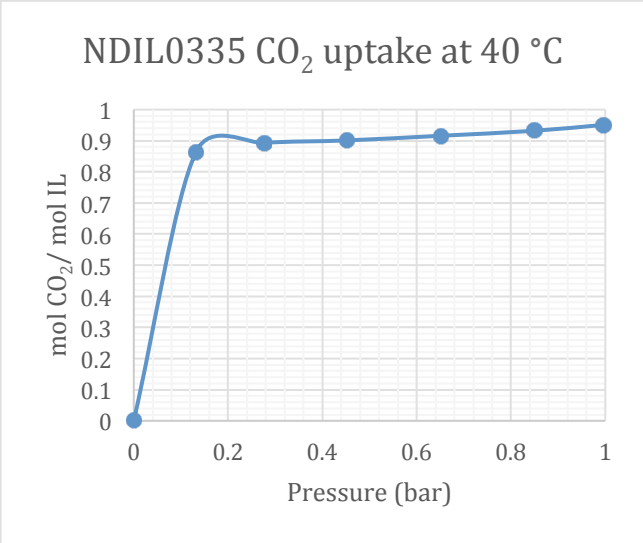

Figure 4: CO_2 uptake at 40 °C for NDIL0335

We also re-measured the CO_2 uptake of samples of NDIL0230 that were sent to LLNL in the first half of 2016. These re-measurements were performed in September 2016. The CO_2 uptake values at 22 °C for samples that were five and seven months old were perfectly consistent with measurements of a fresh sample, as shown in **Figure 5**, indicating that the NDIL0230 samples had not decomposed or degraded in any way.

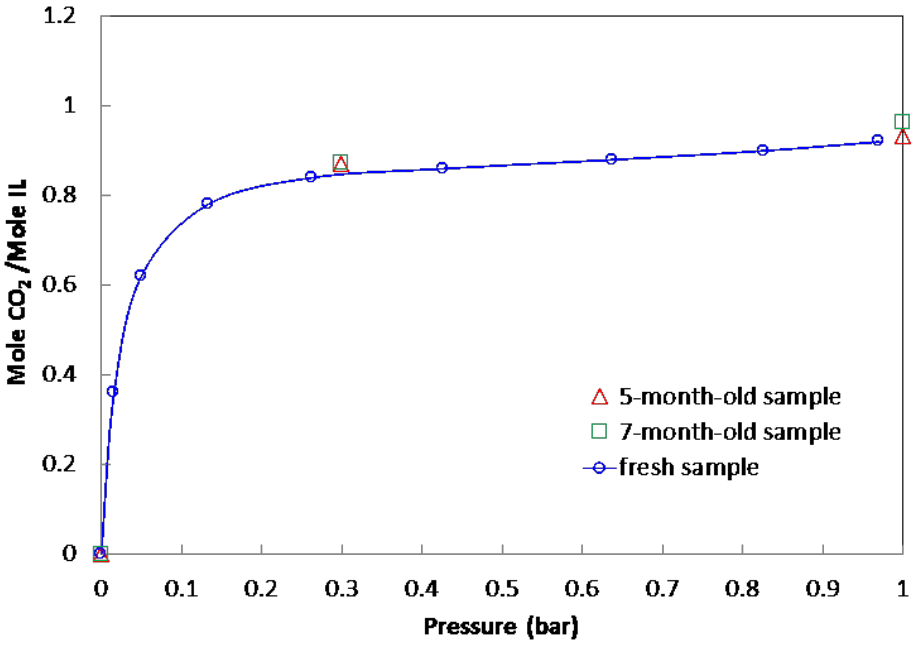

Figure 5: CO_2 uptake at 22 °C of NDIL0230 samples that were five and seven months old, in comparison to measurements with a fresh sample.

Subtask 2.4 - Recyclability testing

In an actual process, the IL and/or PCIL will need to perform for many absorption and desorption cycles. To test this property, we performed cyclic testing (recyclability testing) of our lead candidate material, NDIL0230, to see if we could determine steady-state CO_2 uptake capacity. The NDIL0230 CO_2 uptake recycling was done at room temperature (22 ^oC) using the volumetric apparatus that consists of a CO_2 reservoir and a sample cell of known volumes. The sample was exposed to CO_2 until it was saturated at 1 bar, the uptake was calculated according to the pressure drop inside the sample cell at the equilibrium pressure, as described above. After the sample had reached equilibrium, the ionic liquid was regenerated by heating the sample at 60 ^oC and pulling vacuum for 5 hours. Once the sample had been regenerated, it was exposed again to 1 bar of CO_2. The procedure was repeated 7 times. The CO_2 capacity for this material did not change more than 5% after six cycles, as shown in **Figure 6**.

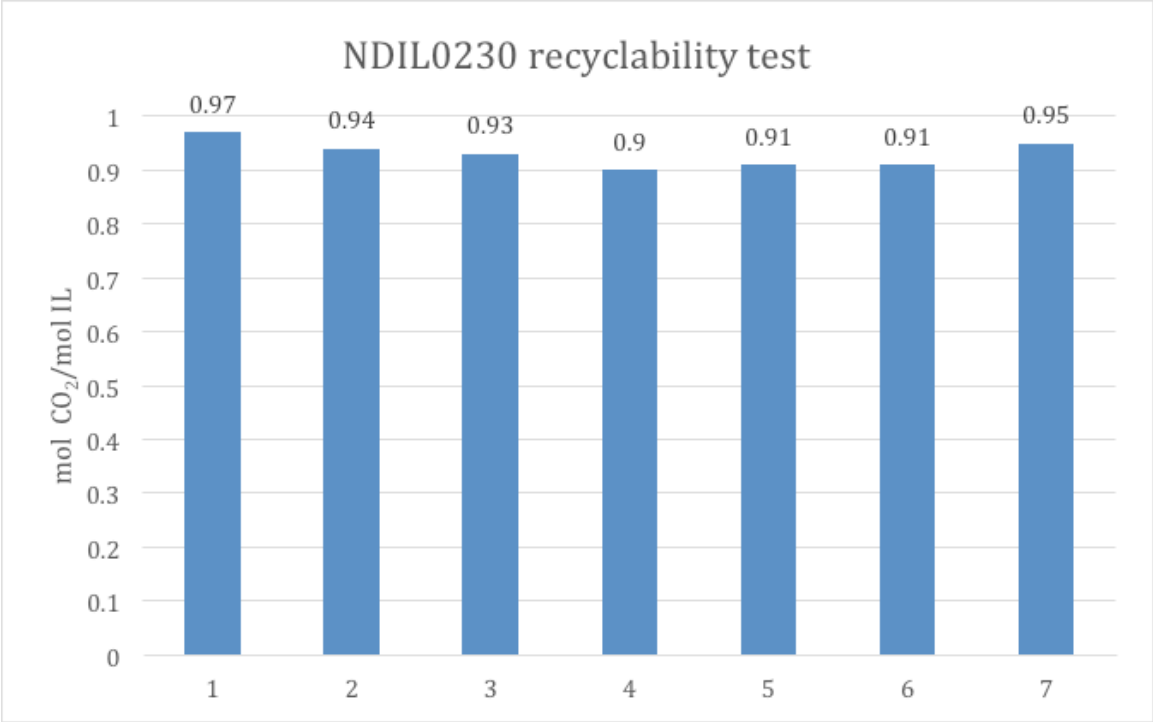

Figure 6: Recycling test for CO_2 uptake of NDIL0230 at 22 °C and 1 bar

In addition, we have tested the recyclability of our lead PCIL candidate material, NDIL0309. The CO_2 uptake recycling was done at 80 ^oC using the volumetric apparatus that consists of a CO_2 reservoir and a sample cell of known volumes. The sample was exposed to CO_2 until it was saturated at 1 bar, the uptake was calculated according to the pressure drop inside the sample cell at the equilibrium pressure, as described in above. After the sample had reached equilibrium the PCIL was regenerated by heating the sample at 80 ^oC and pulling vacuum for 72 hours. Once the sample had been regenerated, it was exposed again to 1 bar of CO_2. The procedure was repeated 6 times. The CO_2 capacity for this material did not drop more than 5% after five cycles (six total uptake measurements), as shown in **Figure 7**.

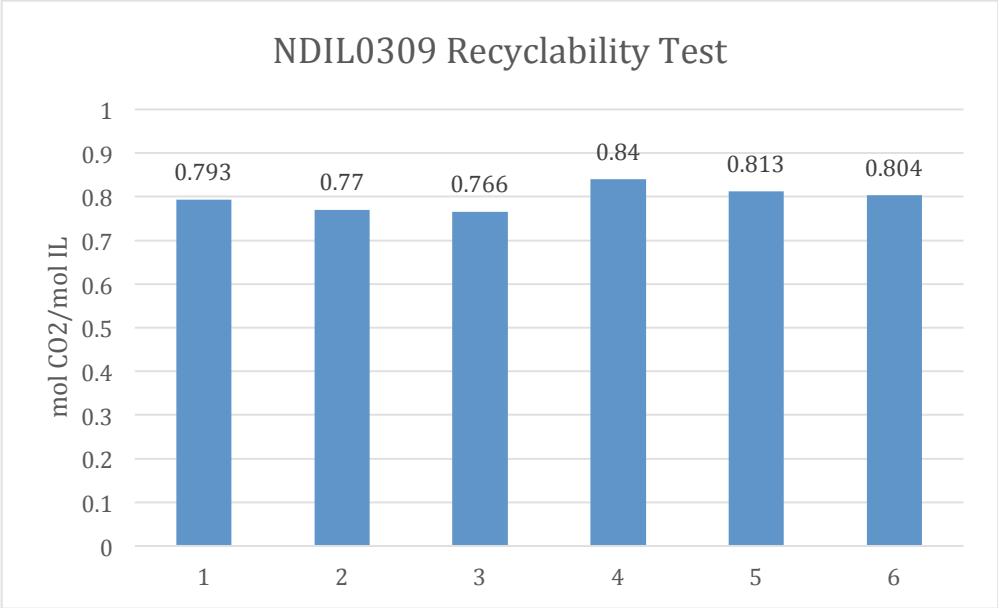

Figure 7: Recycling test for CO_2 uptake of NDIL0309 at 80 °C and 1 bar

We are encouraged by these results, especially if we are able to scale-up the encapsulation of NDIL0230 and NDIL0309 and maintain the same sustained level of CO_2 uptake in cyclic testing of the encapsulated materials.

Subtask 2.5 - Reprotonation equilibrium and kinetics

Since the anions of the IL and PCIL candidates are relatively basic (which is a necessary for them to have sufficient reactivity with CO_2), there is the possibility that they could be reprotonated by water with or without CO_2 present. The general scheme, adapted from Thompson et al., is shown in **Figure 8**.

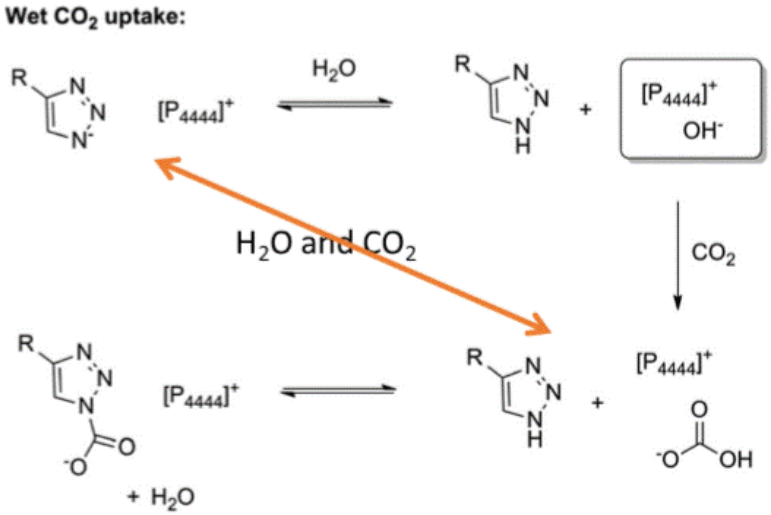

Figure 8: Reprotonation chemistry (adapted from reference **[6]**).

After testing many ideas (including HPLC coupled with a UV-vis detector), we have concluded that NMR analysis is the best general-purpose method to measure reprotonation equilibrium and kinetics. The main pathway of interest is the one shown by the red arrow – the reprotonation of the anion in the presences of both water and CO_2. Using NMR, we have established that NDIL0231 does reprotonate simply in the presence of water (i.e., even without contacting with CO_2). Therefore, we eliminated this material from further consideration. However, using NMR we have shown that the lead IL and PCIL candidates, NDIL0230 and NDIL0309 do not reprotonate just in the presence of water.

However, using NMR spectroscopy, we have determined that both NDIL0230 and NDIL0309 reprotonate very quickly in the presence of both CO_2 and water at room temperature. The results are shown in **Table 6.** The reprotonation equilibrium for NDIL0230 is about 55-60%, whereas the data suggests that at equilibrium the NDIL0309 would be fully reprotonated. The experiments were performed with excess water; i.e., 4 moles of water per mole of IL or PCIL. This is a significantly higher water concentration than one might expect in a post-combustion CO_2 capture process. Nonetheless, the reprotonation occurs very quickly. This suggests that reducing the contact between the IL or PCIL and water, either by pre-drying the flue gas or developing hydrophobic polymer shell materials that selectively exclude water, would be desirable.

Note that at equilibrium NDIL0309 appears to consume more than one mole of water per mole of PCIL. The results are reproducible. We attempted to further elucidate the reaction chemistry using heteronuclear multiple bond coupling two dimensional (HMBC 2D) NMR, but this did not show any unexpected interaction or reaction of the water with other atoms of the PCIL.

Table 6: Kinetics and equilibrium values for reprotonation of NDIL0230 and NDIL0309 at room temperature

	0 sec	30 sec	1 min	2 min	10 min	2 hrs	2 days
NDIL0230	0%	13%	29%	47%	55%		58%
NDIL0309	0%		27%	39%	120%	120%	

The reprotonated anions have very low vapor pressures and, based on their size, it is unlikely that they could diffuse out of the polymer shells. Therefore, if the reprotonation is reversible, it may not be a problem in the CO_2 capture and regeneration process.

Task 3.0 - Encapsulation of ILs

Subtask 3.1 – Identification of IL and PCIL compatible shell materials and/or curing process

Micro-encapsulation is a technique where a material is encased in small (~500 μm diameter), spherical shells of a CO_2-permeable polymer. Micro-encapsulated CO_2

sorbents (MECS) were demonstrated previously with potassium and sodium carbonate solutions. They were shown to increase the rate of CO_2 absorption more than 10-fold and to successfully contain solid precipitates **[7]**. Micro-encapsulation can also address some of the limitations of ILs and PCILs. The purpose of micro-encapsulation of ILs and PCILs is to increase the rates of CO_2 absorption and heat transfer while maintaining the thermodynamic advantages of the IL or PCIL. Secondarily, encapsulation enables phase changes and may slow the uptake of water from wet flue gases.

For this work, MECS are produced in a microfluidic device where the CO_2 capture material and uncured shell material are flowed together in a third, inert carrier fluid through a junction to create double emulsions – drops of CO_2 capture material inside drops of shell material precursor, suspended in the carrier fluid (see **Figure 9**). The shell material is subsequently cured by exposure to ultraviolet light (UV). In this work, capsules are produced in single-junction devices assembled from glass capillaries, but the process can be parallelized for large-scale production.

To successfully produce capsules of a new CO_2 capture material, several criteria must be met: (1) the CO_2 capture material and shell material must maintain a clear interface, (2) the shell material must be able to cure in the presence of the CO_2 capture material, and (3) the cured shell material must be stable in the presence of the CO_2 capture material. For microfluidic production with current techniques, additional practical constraints on the viscosity and interfacial tension of the fluids come into play. Finally, for viable MECS, the shell material must be sufficiently permeable to CO_2 and the capsules must be robust under carbon capture process conditions. These criteria are considered below.

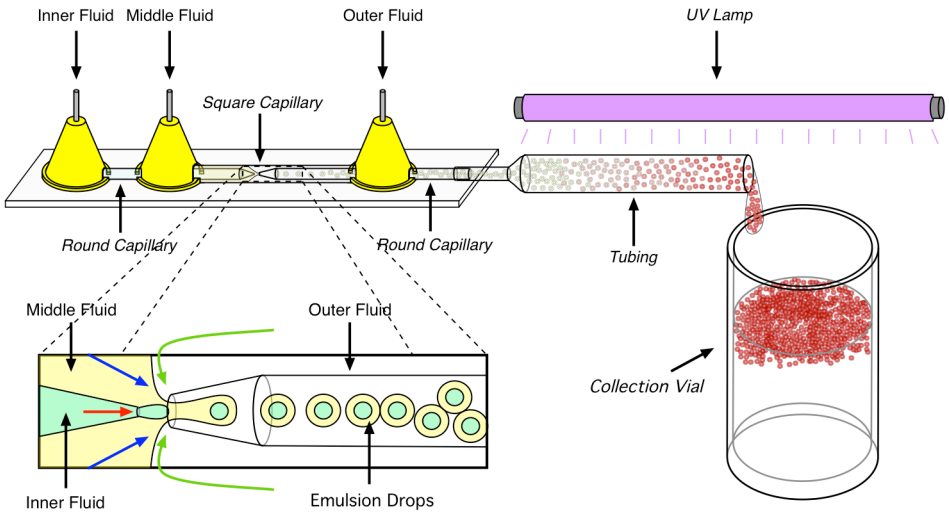

Figure 9: Diagram of the capsule production apparatus. The inner fluid is the IL or PCIL solution, the middle fluid is the shell material precursor, and the outer fluid is an aqueous, inert, carrier solution.

The primary selection criterion for a MECS shell material is high permeability to CO_2. Further criteria include heat stability at the regeneration temperature of the solvent

(typically 80—120°C), mechanical robustness in the chosen process conditions (e.g., fluidized bed), and chemical compatibility with the solvent. For microfluidic production, UV-curable polymers with precursors that are liquid at room temperature are particularly suitable. Silicones have among the highest CO_2 permeabilities of common polymer classes, with typical values on the order of 3000 Barrer **[8]**. After extensive screening and through past and concurrent work on encapsulation, we identified two commercial silicones as promising shell materials for IL and PCIL capsules, Semicosil 949 and Tego-Rad 2650. We also developed two new, in-house formulations, which we term Thiolene and SiTRIS, for capsule screening.

The first is a silicone with a thiolene curing mechanism. Semicosil utilizes a UV-active platinum catalyst to cross-link polydimethylsiloxane (PDMS) polymers via hydrosilylation reactions between vinyl and hydride side-chain/terminal functional groups. In contrast, thiolene based materials take advantage of the radical-mediated reaction between vinyl and mercaptan groups. The thiolene formulation used in the present tests consists of thiol- and vinyl-functionalized PDMS copolymers, a photo-initiator, Irgacure 1173 (2-hydroxy-2-methyl-1-phenylpropane) and reinforcing fumed silica filler (see **Scheme 1**). We measured the CO_2 permeability of the material as 2700 Barrer, which is comparable to the 3100 Barrer measured for Semicosil.

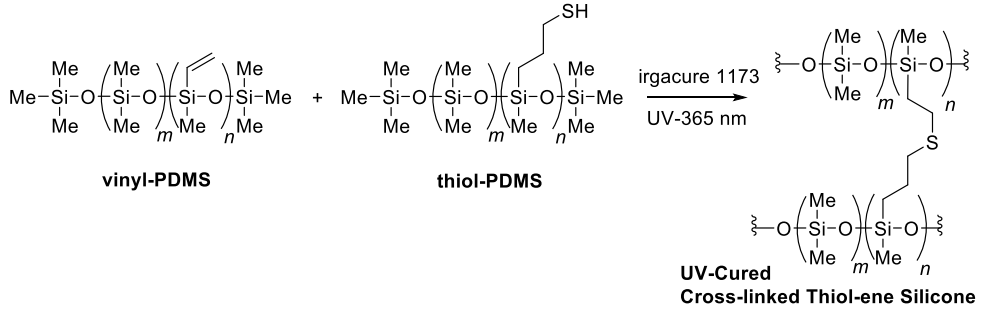

Scheme 1: Formulation of thiolene shell material

The second custom shell material is an acrylate combined with a crosslinking agent and UV activator. 3-[Tris(trimethylsiloxy)silyl)propyl methacrylate (referred to as SiTRIS, see **Scheme 2**) was developed in the early 1970's as a means to enhance the oxygen permeability of contact lens materials. When SiTRIS was mixed with common contact lens monomers, such as methyl methacrylate or hydroxyethyl methacrylate, the relative oxygen permeability was increased 15-fold. Thus, we chose to investigate its use for CO_2 capture. As only linear polymers result from the polymerization of SiTRIS, we added a crosslinker, trimethylolpropane trimethacrylate (TMPTMA), to yield an insoluble, rigid material after curing. Introduction of irgacure 1173 enables UV-curing, with which thin films can be prepared in less than a minute. The measured CO_2 permeability was 400 Barrer, which is high for an acrylate, but substantially lower than our silicone materials. Permeability can perhaps be enhanced by fillers or other modifications currently being investigated.

Active Monomer

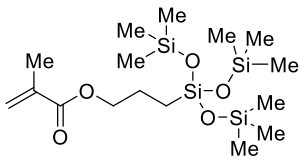

SiTRIS
3-[Tris(trimethylsiloxy)silyl]propyl methacrylate

Crosslinker

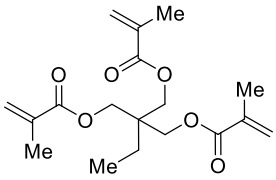

TMPTMA
Trimethylolpropane trimethacrylate

Scheme 2: Formulation of SiTRIS shell material

The shell materials tested in this project are summarized in **Table 7**, showing some of their relevant properties.

Table 7: Summary of shell material candidates with basic properties

Name	Manufac-turer	Material	Permea-bility (barrer)	Amine Compati-bility	Mecha-nical Properties	Curing Time
Semicosil 949	Wacker	Silicone	3100	No	Elastic, strong, tacky	30 mins
Thiol-ene	LLNL	Silicone	2700	Yes	Elastic, strong, tacky	30 secs
SiTRIS (80:20)	LLNL	Acrylic	400	After curing	Stiff, strong, untacky	10 secs
Tego Rad 2650	Evonik	Silicone	3200	After curing	Elastic, friable, untacky	10 secs

	Good properties for encapsulation			Marginal properties for encapsulation		Not compatible			
	NDIL 0274	NDIL 0252	NDIL 0231	NDIL 0231 w/ 1:1 wt.	NDIL 0230	NDIL 0230 w/ 1:1 wt.	NDIL 0309 (solid)	NDIL 0309 w/ 1:1 wt.	Carbon-ate w/ water
Semi-cosil			X	X	X	X			√
Thiol-ene								√	√
Si-TRIS				√		√ w/ 1:3			√
T.R. 2650									√

Figure 10: Summary of IL/shell material compatibility screening tests. "X"s mark unsuccessful capsule production, checks mark successful capsule production.

Following selections described above, we tested five ILs and PCILs for compatibility with shell material candidates. The screening process involves three main tasks: (1) a solubility test, to determine whether the CO_2 capture material would dissolve solid shell material, (2) a test of interfacial stability, to determine if the CO_2 capture material and shell material precursor maintain distinct liquid phases, and (3) a curing test to determine if the shell material cures by UV in the presence of the CO_2 capture material. For promising shell/IL or PCIL pairs, we attempted to produce capsule samples.

NDIL0230 and NDIL0231 appeared very promising for encapsulation in semicosil. However, the neat IL quickly absorbs water during generation, resulting in an aqueous solution, which poisons the polymer (red color). Thus, the attempts to encapsulate neat NDIL0230/0231 failed (marked with X) during in-device test. For NDIL 0230/water in SiTRIS, our in-vial test indicates this IL's 50% water dilution will be hard to encapsulate and was proved true during in-device trial. The encapsulation eventually succeeded when we changed the ratio to 25% IL in water.

Subtask 3.2 – First production of small quantities of encapsulated ILs

Micrographs of four successful capsule batches are shown in **Figure 11 (A-D).** Because NDIL0231 was the lead material at the beginning of the project, we first focused on these capsules. As discussed above, we later eliminated this material as a candidate because NDIL0231 readily reprotonates when contacted with water and its melting point increases when contacted with CO_2. Nonetheless, we successfully produced well-articulated NDIL0231 capsules of approximately 300 μm in diameter using the SiTRIS shell material. In this case, NDIL0231 was diluted 50% in water to reduce its viscosity

during production. The water is later removed by drying. A micrograph of the resulting capsules is shown in **Figure 11A**. We also investigated the applicability of our standard thiolene encapsulation polymer as a shell material. Our initial attempt to encapsulate a sample of NDIL0231 with thiolene was unsuccessful. We determined that there was a compatibility problem between the thiolene polymer and the 50 wt% NDIL0231 – 50 wt% H_2O sample.

Capsules of NDIL0230 were produced in a similar manner, although it was necessary to dilute the IL to 25 wt% initially for stable production, as described above.

NDIL0309 is a PCIL that is in solid powder at room temperature. It was dissolved in water at 50 wt% and encapsulated in our original thiolene mixture (**Figure 11C**). One issue that we noticed about the original thiolene is the added fume silica degrades overnight, resulting in large quantities of aggregated silica in the mixture. This aggregation causes instability in fluid flow and often leads to clogging in the device. However, we cannot simply remove fumed silica as it is needed to improve the mechanical properties. To solve this issue, we reformulated thiolene with a liquid filler (VQM-135 Q resin from Gelest) that will produce more homogeneous mixtures while also maintaining good mechanical strength. The resulting "thioleneQ" mixture was used to encapsulate NDIL0309 and successfully produced capsules with thinner shells and better stability (**Figure 11D**). These capsules were then cleaned and dried with the same method aforementioned to remove water and initially absorbed CO_2. Because the un-encapsulated NDIL0309 is a solid powder, it was also left on a mesh stack and tested like capsules. The comparison of the absorption rate of encapsulated NDIL0309 to pure solid powder NDIL0309 is shown in **Figure 14.** Note that the encapsulated NDIL0230, NDIL0231 and NDIL0309 have varied and unknown amounts of water present, which reduces the viscosity compared to the pure ILs and PCIL. Capsules do appear to absorb faster than un-encapsulated powder, but not at an enhancement that we typically see in previous measurements when comparing capsule to a 1 mm deep stagnant liquid pool. This is likely because of NDIL0309's powder form, which creates much higher surface area than a typical liquid pool, reducing the surface area enhancement provided by the capsules. However, we should note that NDIL0309 is very hygroscopic at ambient conditions and easily becomes a liquid solution when exposed to the environment. Therefore, the CO_2 absorption rates in the figure are not comparable because the encapsulated NDIL0309 may be an aqueous solution rather than a solid. The significant energy reduction for the PCIL cannot be realized if the PCIL is used as an aqueous solution, which may be the situation for the CO_2 uptake rates shown in the figure for the encapsulated NDIL0309.

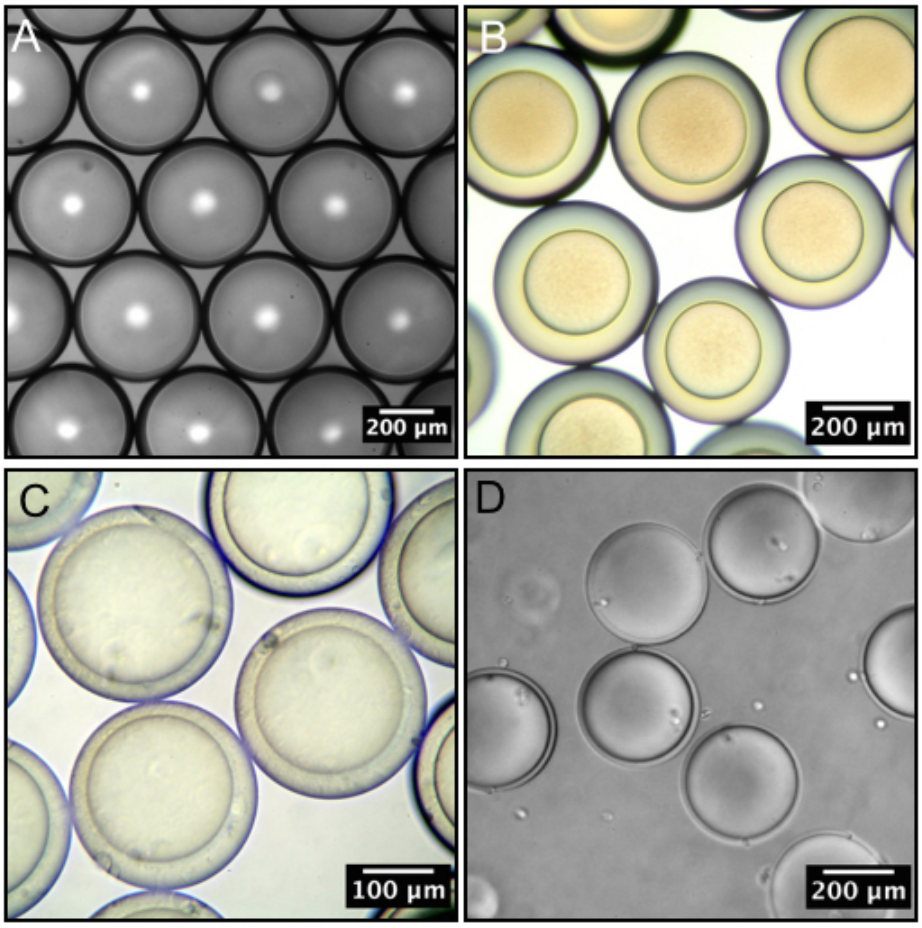

Figure 11: Successful microcapsules. A: NDIL0231/water-in-SiTRIS. B: NDIL0230/water-in-SiTRIS. C: NDIL0309/water-in-thiolene. D: NDIL0309/water-in-thioleneQ.

To measure CO_2 absorption rates, capsules are loaded onto wire mesh trays (**Figure 12**), rinsed with DI water repeatedly, dabbed with a Kimwipe, and heated on a hot plate in air at 60°C for 6 hours to remove water and CO_2. A control sample of liquid solvent is diluted with water and similarly heated to dryness in an open beaker. Dried capsule and CO_2 capture material samples each have a mass of about 0.5 g. The trays or beaker are then placed inside a pressure-drop apparatus for measuring gas absorption (see Vericella et al **[7]**). The chamber is evacuated to about 0.01 atm total pressure and then pressurized to about 0.19 atm with pure CO_2. By monitoring total pressure over time, the rate of CO_2 absorption is inferred. The chamber temperature was maintained at 25 °C.

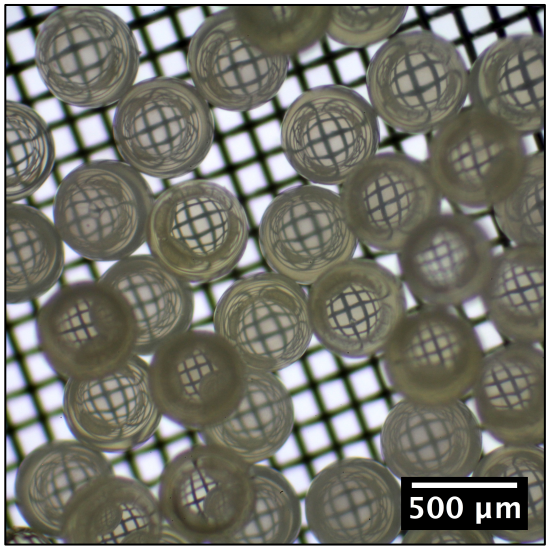

Figure 12. Photograph of dried NDIL0231-SiTRIS microcapsules on metal mesh.

Pressure data are collected in time series and then converted to CO_2 absorbed and CO_2 absorption rate. An example is shown in **Figure 13**. Taking the average absorption rate over the first minute, we compare rates among three types of capsules produced so far. These are compared with the rate for sodium carbonate capsules from the literature. See **Figure 14**.

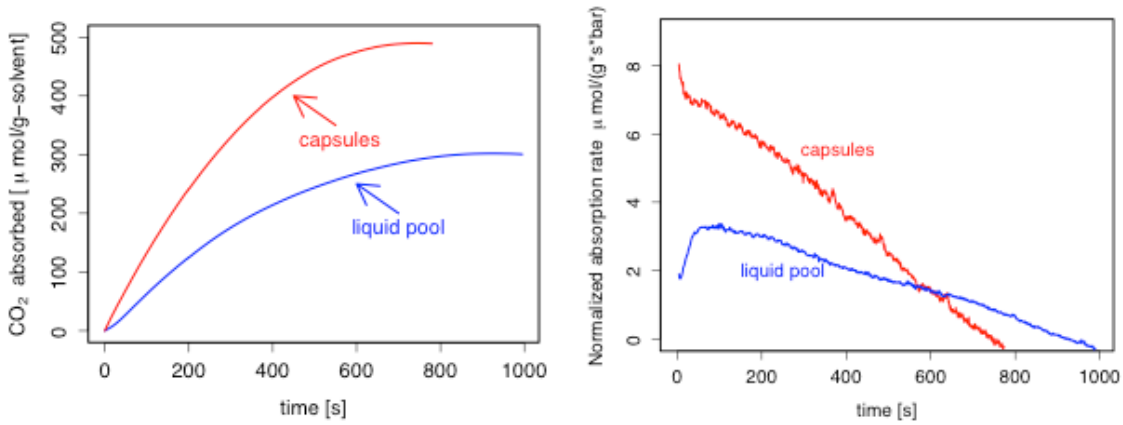

Figure 13: CO_2 absorbed (left) and normalized absorption rate (right) over time by NDIL0231 with and without encapsulation. The rates are normalized by mass of solvent and partial pressure of CO_2.

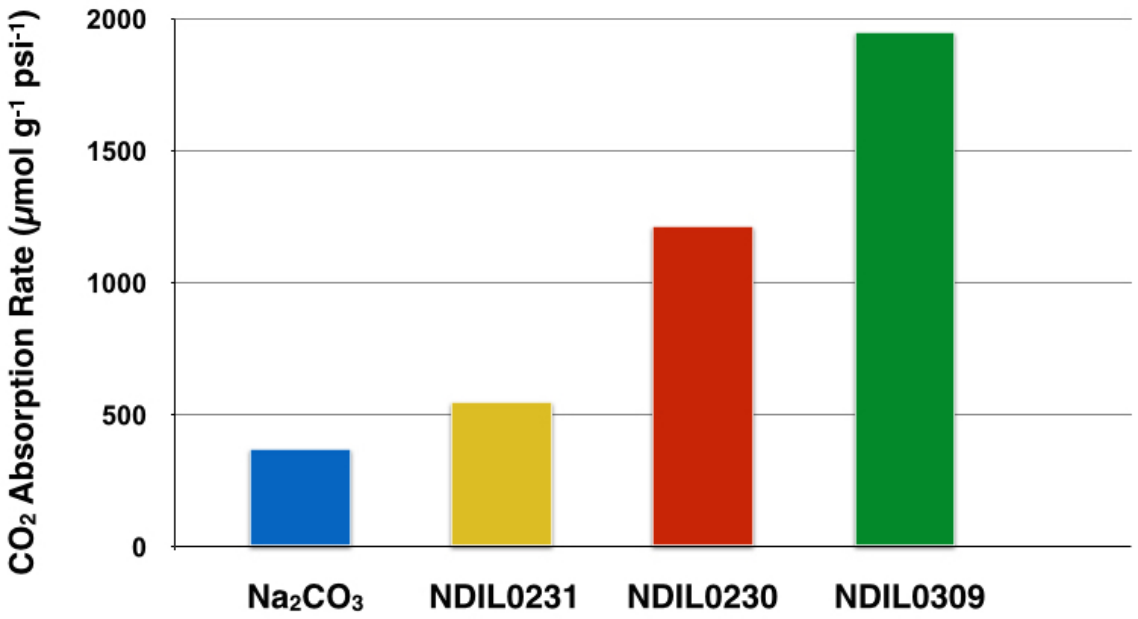

Figure 14: Initial CO_2 absorption rates for four types of encapsulated solvents.

Subtask 3.3 – Production of a suite of small quantities of encapsulated ILs

To date, Notre Dame has received ten samples, totaling approximately 22 grams from LLNL, about 10 grams of which were encapsulated IL or PCIL. A complete list of the samples provided by LLNL for Notre Dame's evaluation, is included as **Table 8.**

Table 8
Capsule Samples Received by Notre Dame from LLNL

Date Sent	No. of Vials	Amount	Description
April 19th	1	~1 g	NDIL0231-SiTRIS capsules. Core fluid starts with NDIL0231 w/ 50wt% water. Dry on hot plate/fume hood-> absorb CO2 -> regenerate on hot plate/fume hood
	1	~1 g	Same capsule batch, dry->absorb CO2->seal in vial directly
	1	~0.5 g	Same capsule batch, as-is right after capsule shell cross linking-stored in osmotically balanced water/glycerol/polyvinyl alcohol mixture
May 12th	1	~2 g	NDIL0230-SiTRIS capsules. Core fluid starts with NDIL0230 w/ 75 wt% water. Dry on hot plate/fume hood, no CO2 absorption test was carried out.
	1	~2 g	NDIL0309 -Thiolene capsules. Core fluid starts with NDIL0309 w/ 75 wt% water. Dry on hot plate/fume hood, no CO2 absorption test was carried out
July 7th	1	~4.0 g	NDIL0230-SiTRIS capsules. Core fluid starts with NDIL0230 w/ 75 wt% water. Dry on hot plate/fume hood, no CO2 absorption test was carried out.
	1	~0.5 g	Hollow SiTRIS capsules for control study. Dry on hot plate/fume hood
August 26th	1	~7 g	Aqueous Na_2CO_3 in TegoRad2650 capsules
	1	~ 2g	Glycerol-SiTRIS capsules
	1	~ 2g	Carbonate-TR2650 capsules dusted with fumed silica

Task 4.0 - Testing of Encapsulated IL Particles

Subtask 4.1 - Thermodynamic testing

We performed the measurements of the CO_2 uptake of several encapsulated IL samples. For the first sample tested, NDIL0230 in SiTRIS at 22 °C, the CO_2 uptake was significantly below the uptake values of the bulk NDIL0230. We then measured the CO_2 uptake of the SiTRIS encapsulated NDIL0230 at two additional temperatures, 40 and 60 °C, as shown in **Figure 15**. Obviously, the CO_2 uptake is significantly lower than expected. Note that the comparison is made using the weight percent of NDIL0230 based on the flowrates used in the microfluidic device at LLNL assuming that the NDIL0230 was pure. This assumption may not be completely correct since the IL sample was exposed to the atmosphere, which will result in water absorption, and the water content of the NDIL0230 sample was not measured at LLNL prior to encapsulation.

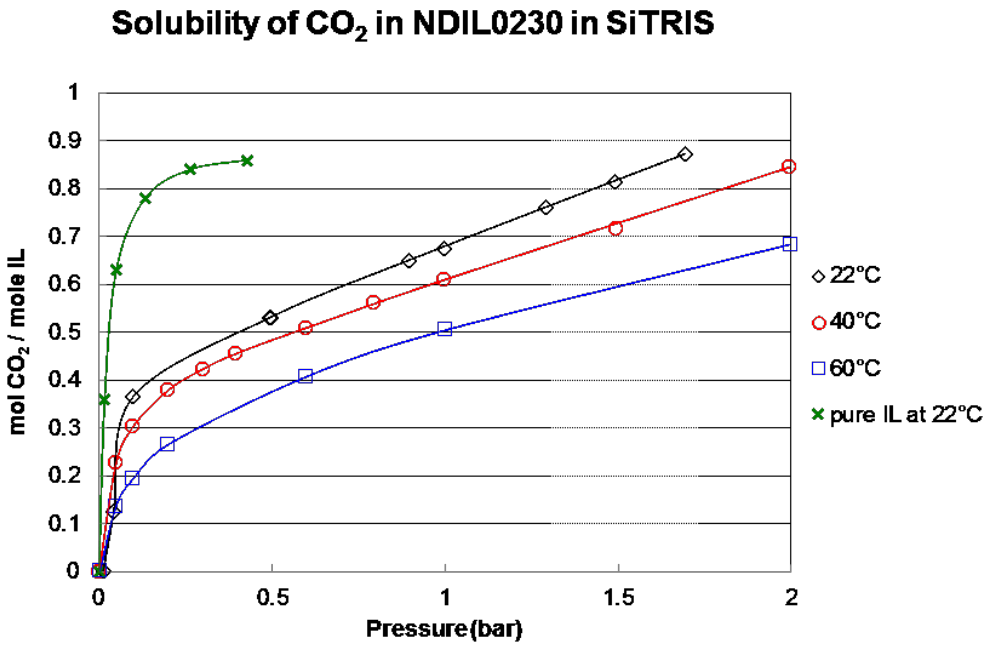

Figure 15: Solubility of CO_2 in SiTRIS encapsulated NDIL0230 – batch 1.

Subsequently, we received an additional batch of NDIL0230 encapsulated in SiTRIS from LLNL and measured the CO_2 uptake of that sample. Those results are shown in **Figure 16**. The CO_2 uptake for this sample was much higher, closer to the anticipated values. The difference in the samples is that Batch 1 was made with unoptimized conditions where the polymer precursors were in contact with the IL for long periods of time prior to polymerization and cross-linking. By contrast, Batch 2 was made with optimized conditions and shorter contact between the IL and the polymer precursors.

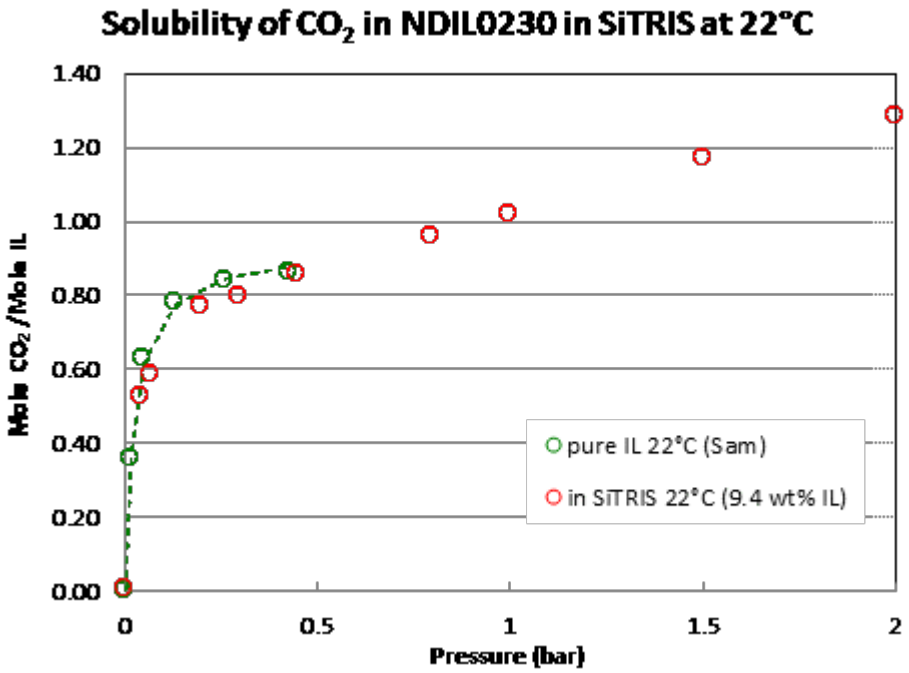

Figure 16: Solubility of CO_2 in SiTRIS encapsulated NDIL0230 – batch 2.

However, both batch 1 and batch 2 of NDIL0230 encapsulated in SiTRIS showed significant CO_2 uptake with increasing pressure (e.g., above 1 bar). To investigate the cause of this increase, we measured the CO_2 uptake of hollow SiTRIS shells at 22, 40 and 60 °C. Those results are shown in **Figure 17**.

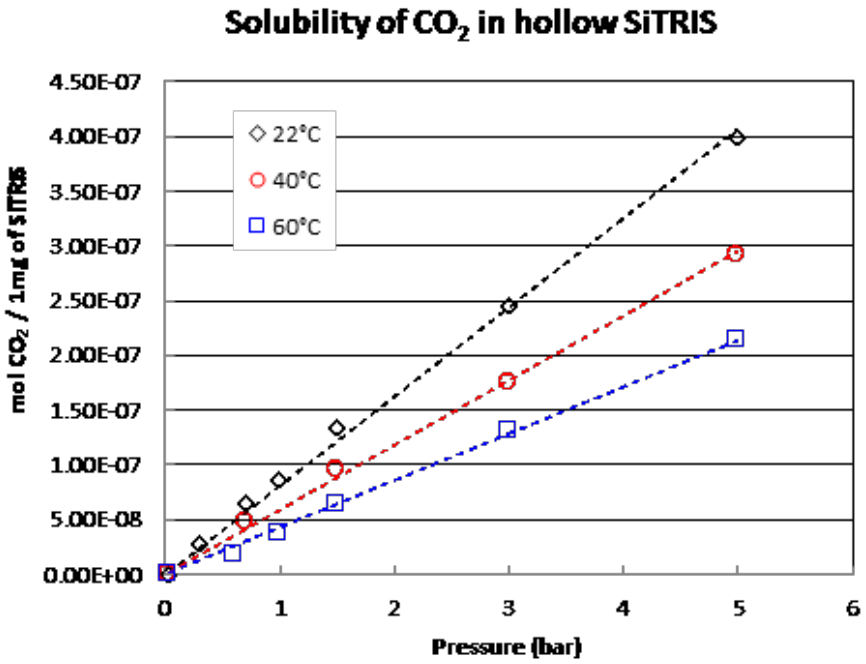

Figure 17: Solubility of CO_2 in the SiTRIS polymer.

Even though this is just physical dissolution of the CO_2 in the polymer, it can make a substantial contribution to the overall CO_2 uptake because the shell material is such a large part of the total mass of the particles. For instance, for Batch 2 of the NDIL0230 in SiTRIS shells, the IL is estimated to be only 9.4 wt%, with the polymer being 90.6 wt% of the total mass. When the CO_2 uptake due to physical dissolution in the polymer shell material is subtracted from the total uptake, the uptake of CO_2 by the NDIL0230 is shown in **Figure 18.**

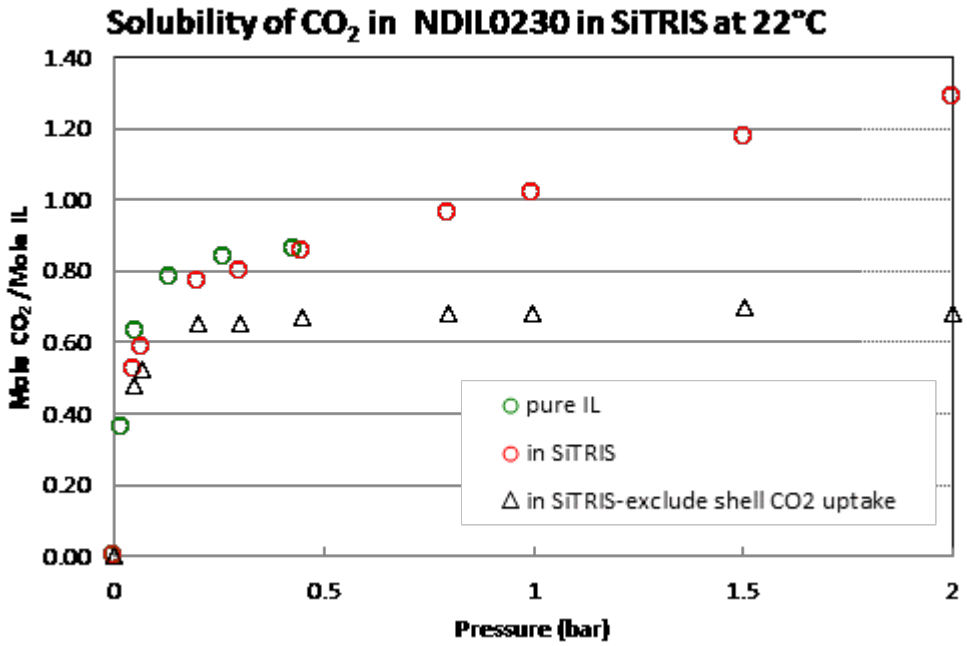

Figure 18: Solubility of CO_2 in SiTRIS encapsulated NDIL0230 – batch 2 – after the uptake by the shell material has been subtracted from the total uptake.

As seen in the figure, when the CO_2 uptake by the polymer is excluded, the uptake by the NDIL0230 is well below the uptake by the pure bulk IL.

In order to investigate the cause of the lower CO_2 capacity, we broke open some of the SiTRIS encapsulated NDIL0230 capsules, both batch 1 and batch 2, and analyzed the contents by NMR spectroscopy. NMR showed that NDIL00230 has reacted with the SiTRIS precursor and that the degree of reaction was greater for batch 1 than batch 2. From this we concluded that NDIL0230 was not compatible with SiTRIS. Subsequently, we have tested the compatibility of NDIL0230 and NDIL0309 with various commercial polymer precursor materials provided by LLNL, as shown in **Table 9**. The conclusion is that SiTRIS is not compatible, but that the Thiolene is compatible. The TegoRad may be a possibility.

Table 9: Compatibility of polymer and polymer precursors with IL and PCIL candidates. Red indicates incompatible, green indicates compatible and yellow indicates possible compatibility.

	NDIL0231	NDIL0230	NDIL0309
TRIS			
SiTRIS Beads			
New SiTRIS			
SMS			
DMS-V			
Tego Rad 2300			
Tego Rad 2560			
Irga 11173			
TMPTMA			
Thiolene beads			

In addition, we measured the CO_2 uptake by NDIL0309 encapsulated in thiolene at 60, 70 and 80 ^oC. These results are compared to the pure NDIL0309 uptake in **Figure 19**. If the NDIL0309 content of the spheres is 19.4 wt% (which is what is shown in the figure), then the encapsulated NDIL0309 has capacity consistent with the bulk material. NMR analysis of the shell contents suggests that the NDIL0309 content is about 22 wt%, whereas the flowrates in the microfluidic device at LLNL suggests 25 wt% if the NDIL0309 is 100% PCIL. However, LLNL has subsequently shown by TGA that the NDIL0309 as used at LLNL contains a significant amount of water. This is due to the hygroscopic nature of the ILs and PCILs. If exposed to the atmosphere they will absorb water, with the amount of water absorbed dependent on the relative humidity and time of exposure.

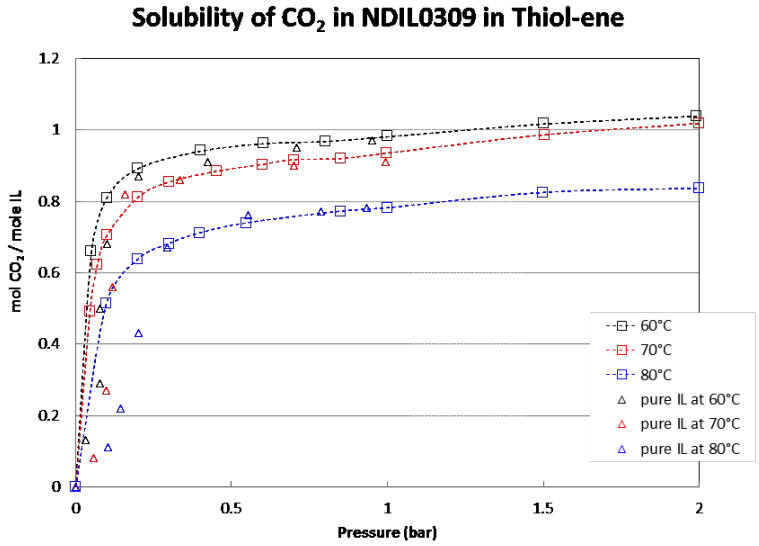

Figure 19: Solubility of CO_2 in thiolene encapsulated NDIL0309, assuming 19.4 wt% active material.

Subtask 4.2 – Mechanical and dynamic particle property testing

The capsules tested as part of this Subtask were specifically made by LLNL for fluidization durability testing. They have SITRIS shells and were filled with glycerin. We examined these using a light microscope with several different light filters (**Figure 20**). The diameter of the particles ranged from 250-280 um and all appeared to be without significant defects before tests.

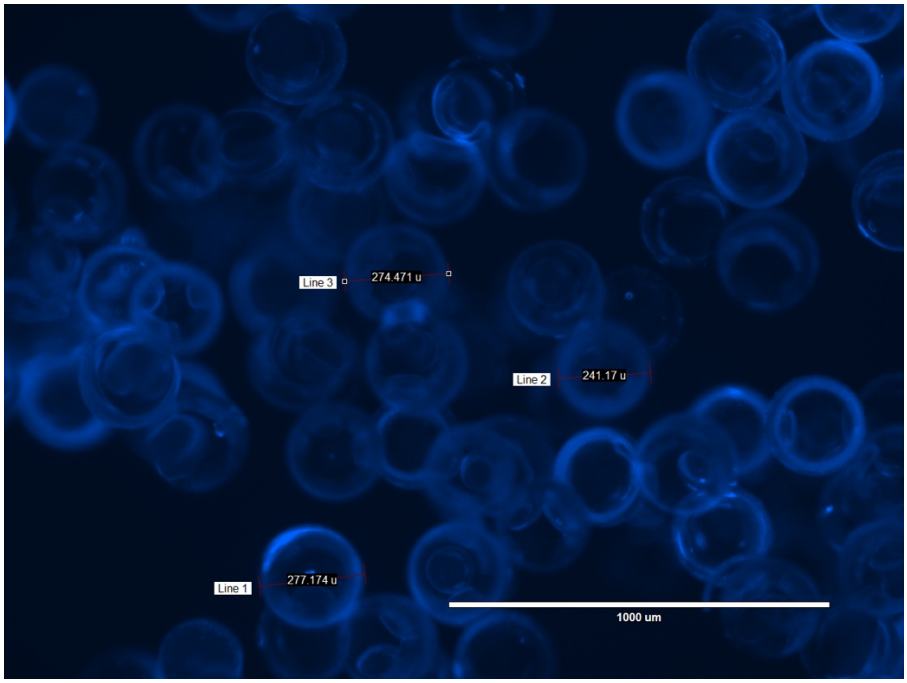

Figure 20: Photo of encapsulated glycerin shows very uniform and consistent particles

These particles were fluidized for 19 hours with some removed for observation after 10 min, 1 h, 3 h, 11 h, and 19 h. Very little change in the particles occurred over the course of the experiment. A small fraction was slightly dented, perhaps due to particle collisions, but no evidence of rupture or loss of integrity was observed (see **Figure 21**).

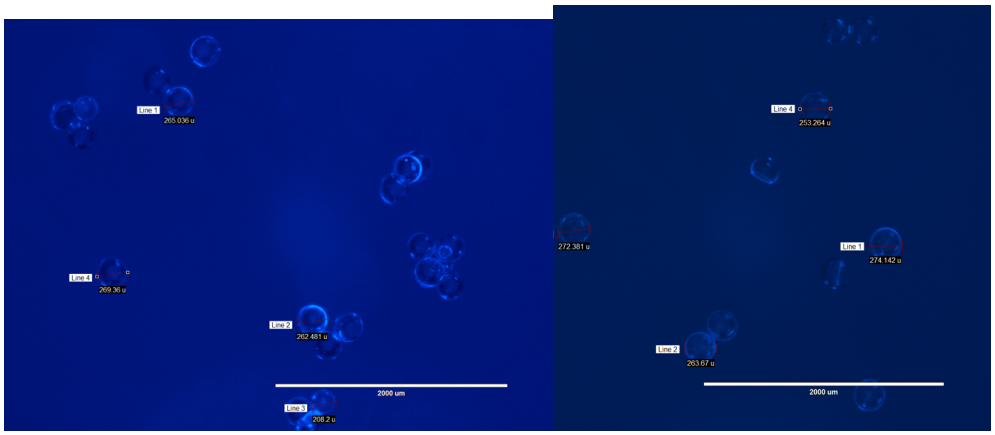

Figure 21: left and right: A sampling of capsules after fluidization for 19 hours. No evidence of significant degradation is seen.

Task 5.0 – Development of a Rate-Based Process Model

Subtask 5.1 - Rate-based model for IL liquid/gas packed bed absorber

We developed a detailed rate-based absorber model that will be used for absorber sizing and performance evaluation. Our model is based on the relevant transport properties of ILs. This model of a standard packed-bed, IL-based absorber will be used to provide a baseline with which to compare the performance of the novel micro-encapsulation-based absorber technology.

On a fundamental level, gas absorption in a packed column is quite complex, in that it involves several simultaneous types of interactions between gas and liquid phases, which can be described in terms of thermodynamics, hydrodynamics, mass transfer and chemical reaction kinetics. In order to obtain a bulk level approximation of absorber performance, it is a common approach to imagine the absorber as consisting of a series of "transfer units," whose number, height, and cross-sectional area can be determined based on fundamental gas and liquid properties and on the absorber design. Based on this scheme, our rate-based absorber model is comprised of three modules: NTU (Number of Transfer Unit), HTU (Height of Transfer Unit) and Hydraulics (for cross-sectional area).

The NTU reflects the concentration driving force, or departure from equilibrium, between the gas and liquid phases and so is based on thermodynamic considerations. The HTU reflects the efficiency of mass transfer between the phases, and so is based on kinetic considerations. The cross-sectional area reflects hydraulic considerations, namely the approach to the hydrodynamic limit (flooding condition). As an example of the type of study that can be done using the model, **Figure 22** shows the effect, for several types of packing, of IL viscosity on the volume of a transfer unit (VTU), which reflects both mass transfer rate (HTU) and cross-sectional area (Hydraulics). It should be noted that a low VTU does not necessarily indicate the best type of packing. In this case, the low-VTU

packings provide high surface areas and thus high mass transfer rates, but at the expense of higher resistance to flow in the column, necessitating impractically large cross-sectional areas. These calculations were done for the case of a 550 MWe (net) subcritical pulverized coal power plant, with flue gas flow rate of 760 m^3/s (Case 10 in Yang et al. [**11**])

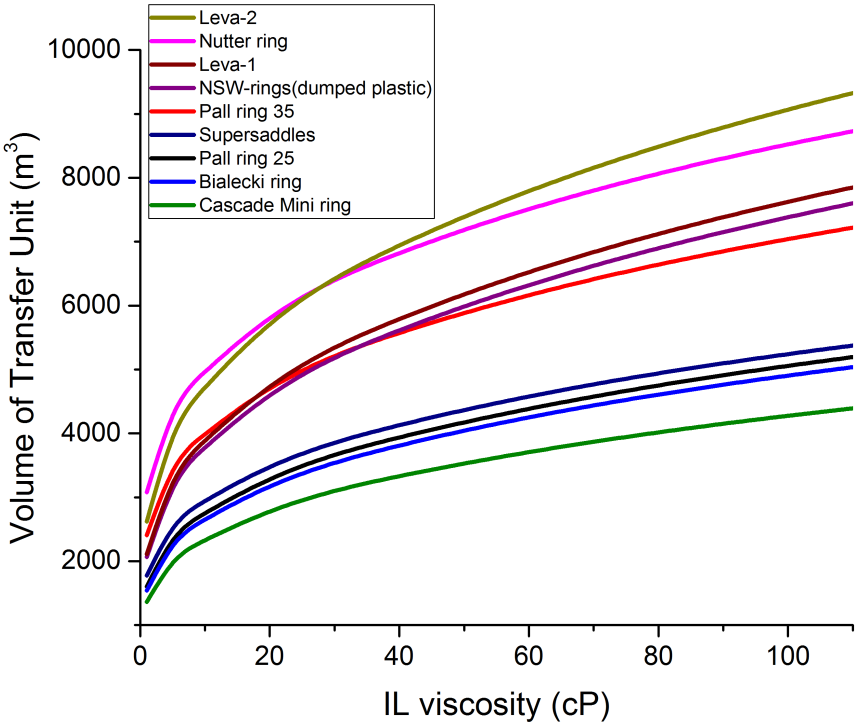

Figure 22: VTU vs. IL Viscosity

Subtask 5.2 - Rate-based model for fluidized IL microcapsules

We developed a rate-based model for a circulating fluidized bed of microencapsulated ionic liquid. This model is for the case of a typical riser-type fluidized bed, with microcapsules flowing upwards and removed from the top of the bed for circulation and regeneration. The model can be used to relate fluidized bed performance to process parameters, microcapsule properties and IL properties. For example, **Figure 23** shows the fluidized bed performance, in terms of the rich (solid) phase CO_2 loading, for different values of the exit voidage ε_{ex} and a microcapsule diameter of 200 μm, as a function of the enthalpy of absorption of CO_2 by the IL, with comparison to the saturation rich and lean values at the indicated absorber and stripper conditions. **Figure 23** suggests that the more negative the absorption enthalpy, the higher the CO_2 uptake for both lean loading and rich loading. This, as shown in **Figure 24** results in a low CO_2 absorption rate due to the shortage of unreacted IL. However, **Figure 24** also indicates if the binding energy is too weak (less negative) then the reaction equilibrium becomes unfavorable and thus there is a lower CO_2 diffusion driving force between the gas phase

and liquid core, resulting in a lower overall mass transfer rate. This trend is directly reflected in **Figure 25** (in terms of reactor productivity, the rate of CO_2 absorption per unit reactor volume) due to the direct link between mass transfer rate and reactor productivity. Additionally, it is seen in **Figure 25** that smaller capsules provide a larger gas-solid contacting surface area, and therefore, have lead to reactor productivity. For a capsule diameter of 200 μm, the highest productivity is around 0.53 mol/(m^3 s). This is close to the reported productivity for an MEA-based packed column **[10]**. However, a fluidized bed reactor is still considered preferable since expensive packing materials are not required, which results in a cheaper unit reactor volume.

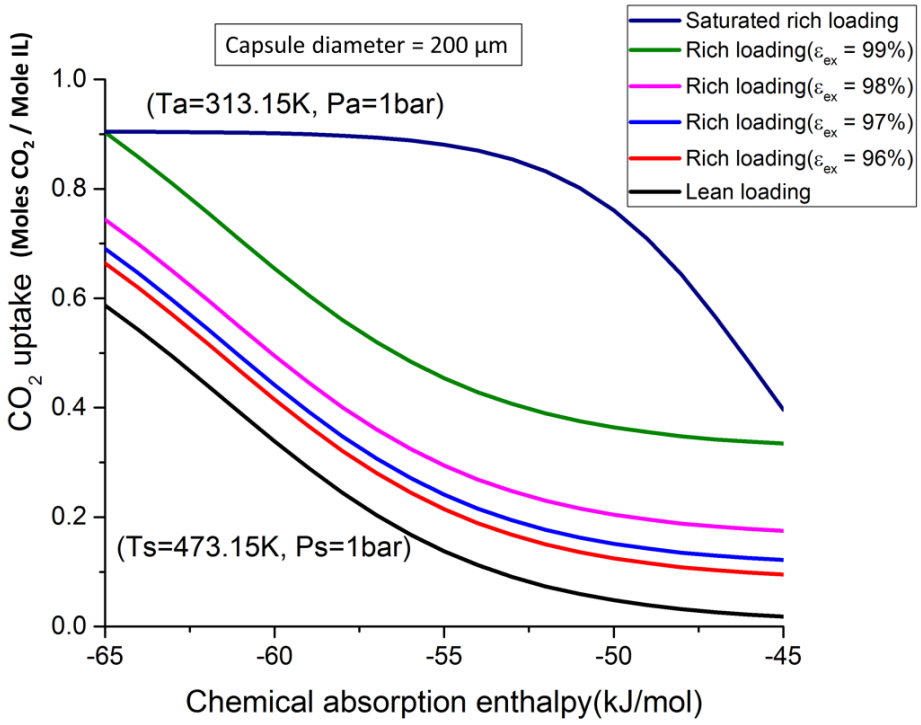

Figure 23: fluidized bed performance, in terms of the rich (solid) phase CO_2 loading, for different values of the exit voidage ε_{ex} and a microcapsule diameter of 200 μm, as a function of the enthalpy of absorption of CO_2 by the IL, with comparison to the saturation rich and lean values at the indicated absorber and stripper conditions.

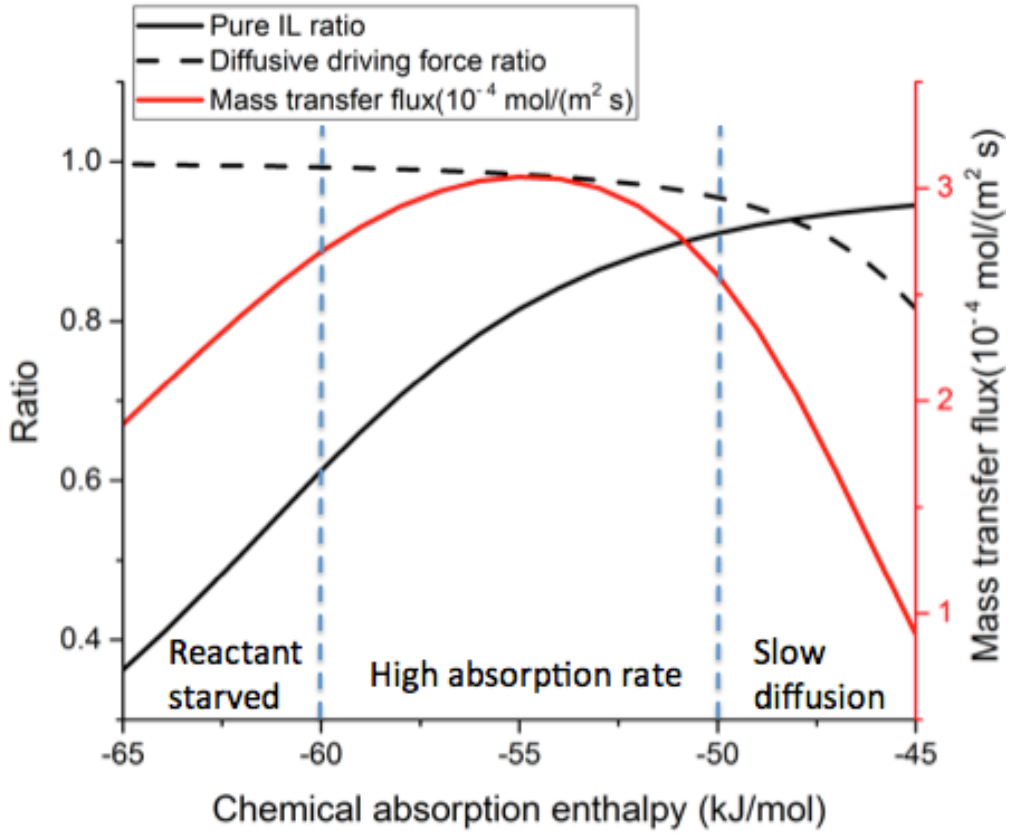

Figure 24: Fluidized bed performance (at $\varepsilon_{ex} = 0.99$, $d_p = 200$ μm), in terms of mass transfer flux of CO_2 from gas phase to liquid core, as well as the profiles of unreacted to total IL ratio C_{IL}/C_{IL}^0 and diffusive driving force ratio $(y_{CO2} - y_{CO2}^*)/y_{CO2}$ (where y_{CO2} is the mole fraction of CO_2 in the gas phase, and y_{CO2}^* is the mole fraction of CO_2 in the bulk liquid core at the chemical equilibrium state).

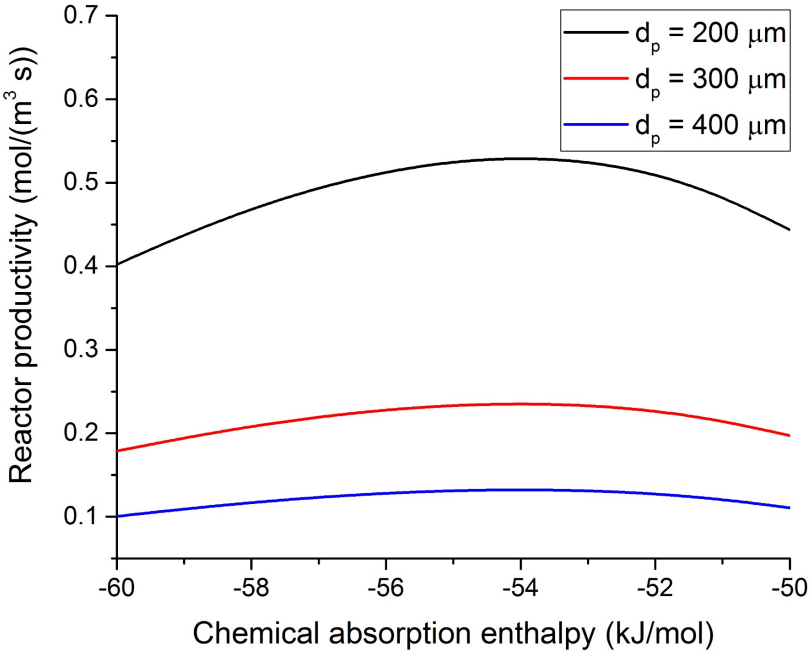

Figure 25: Fluidized bed performance (at $\varepsilon_{ex} = 0.99$), in terms of reactor productivity, the rate of CO_2 absorption per unit reactor volume, at the capsule diameters of 200 μm, 300 μm and 400 μm.

Subtask 5.3 - Rate-based model for packed bed of IL microcapsules

For a static packed bed of solid sorbents, it has been noted **[12]** that heat dissipation from the exothermic sorption reaction and heat transfer to the solid sorbents for the endothermic regeneration will produce local "hot" and "cold" spots, respectively, preventing efficient conversions. The same problems can be anticipated in a static packed bed of IL microcapsules. This issue can be tackled by using bubbling fluidized bed reactors, which can enhance the heat transfer among particles and thus eliminate the local hot/cold spots. Note that in this situation, unlike that of the previous section, there is no circulation of the fluidized particles, which are kept in a bubbling state of fluidization.

In developing our model, we assumed a batch, temperature-swing process consisting of two batch reactors. For a single reactor, the bed (at a capsule diameter of 200 μm) is first fluidized by the flue gas flow and CO_2 is absorbed; then CO_2 is desorbed to regenerate the bed by purging the bed with a hot CO_2 stream until the predefined regeneration temperature is reached. Finally, the bed is purged with cool air for reducing the reactor temperature to the original absorption temperature. The alternation of absorption and desorption modes between the two reactors allows the flue gas to be processed in a continuous manner, as shown in **Figure 26**. This leads to the constraint that the absorption time should be equal to the sum of desorption and cooling times, which can be

estimated by using a dynamic heat transfer model. Once the absorption time is known, the overall mass transfer rate, the bed volume and the reactor volume can be calculated by solving the rate-based material balance equations. The total heat requirement can then be estimated using the known bed volume. **Figure 27** shows results for the case of the absorption and regeneration temperatures fixed as 323.15°K and 433.15°K, respectively, again based on Case 10 in Haslbeck et al. **[9]**. The indicated heat requirement is significantly higher than figures that have been given **[12]** for MEA-based carbon capture technology (120.1 MWe). This reflects an inherent energy-inefficiency due to the need to alternately heat and cool the reactor beds **[11]**. This is especially the case for high heat capacity sorbents like ionic liquids. An additional issue of importance is that to sustain the bubbling state of fluidization in the bed, the gas velocity must be kept strictly below the particle terminal velocity (and thus less than the gas velocity possible in the circulating fluidized bed). Because of this limitation on the gas velocity, high cross-sectional areas will needed, leading to a very large footprint when processing the flue gas from commercial-scale power plants. We consider the circulating fluidized bed, as modeled to be a more promising processing alternative.

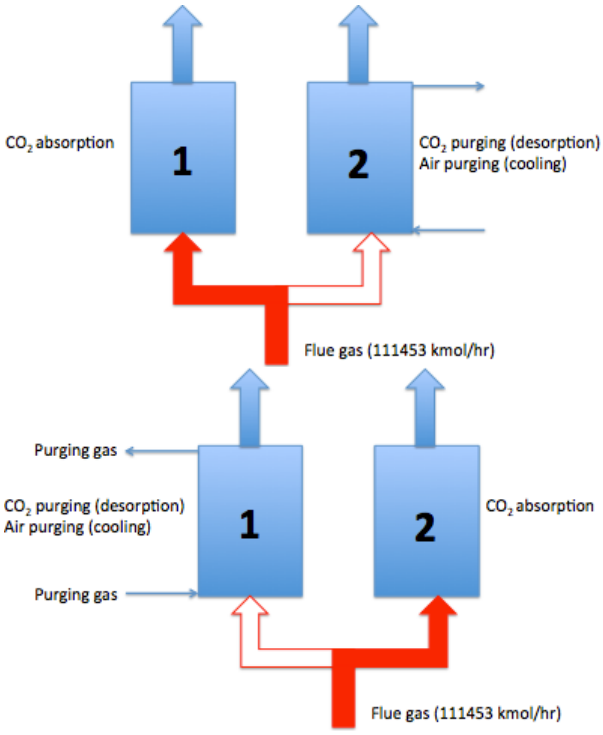

Figure 26: Schematic of the absorption-desorption cycle in a batch, temperature-swing carbon capture process.

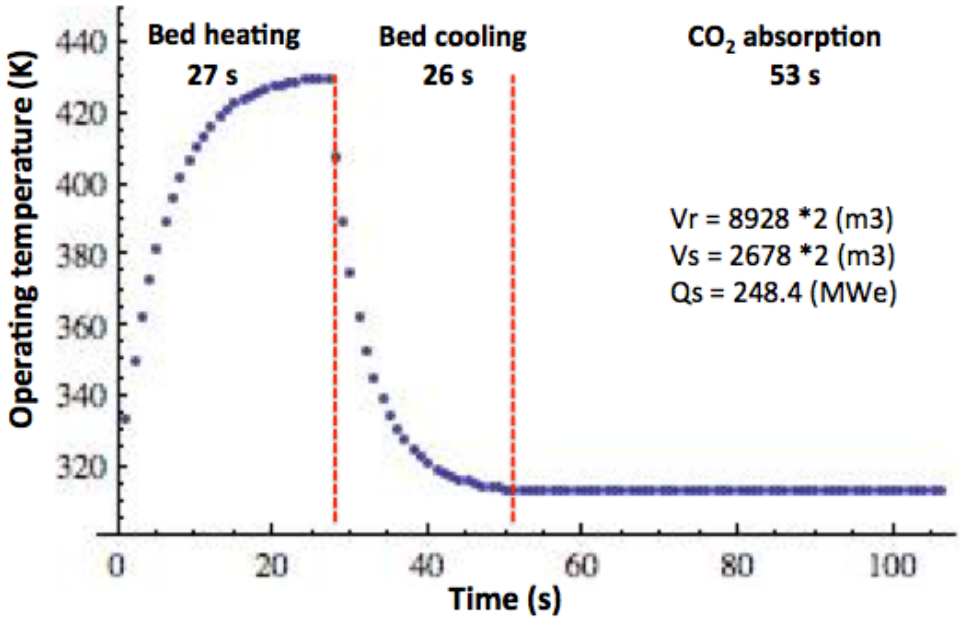

Figure 27: Profile of reactor temperature obtained by solving the dynamic heat transfer model. Also indicated are the total reactor volume V_r, the solid bed volume V_s (assuming void fraction of 70%), and the total heat requirement Q_s (assuming 90% recovery of heat from the heated air generated during bed cooling).

Task 6.0 - Design of Laboratory Scale Testing Unit

Subtask 6.1 - Design of fluidized bed absorber

We developed a simplified reaction-diffusion model to estimate the rate of transport for CO_2 within the particles. Using the most recent measurements of the "shell" transport rates, we found that the primary mass transfer resistance is in the core where the CO_2 diffuses, and then reacts with the ionic liquid. Most importantly, we find that the IL-CO_2 reaction has the advantage of greatly increasing the absorption capacity over what could be obtained by physical absorption. However, to fully saturate the capacity, contact times of a few minutes will be needed. This compares to only a few seconds for the time scale of the shell. As part of our design program, our experimental fluidized bed rig has been re-sized to accommodate the small amount of particles that will be available during the first year of experimentation.

The capsules that are produced by LLNL have diameters of 300 – 600 μm. We expected (and later confirmed) that we would get incipient fluidization with superficial velocities of 5-10 cm/s. The range of operation of the fluidized bed should be up to at least 100-300 cm/s, which is the settling velocity of particles of this size.

Our original thought was that the experimental facility would accommodate gas flow rates for column sizes of 2-5 cm. From our regular meetings of the entire group of researchers, it became apparent that if we could accommodate smaller samples of capsules, we could test many more formulations of inner ionic liquid and shell material.

So we picked flow meters that allow us to use columns as small as 0.5 cm for initial tests. Once the best formulations are identified, we will use larger quantities of capsules and make sure that we have a column diameter large enough to make wall effects negligible.

A key question in the design is what quantity of capsules and what range of gas flows can be used that will allow an accurate measurement of the concentration change across the bed and hence allow calculation of the mass transfer rates. To determine this, we developed a reaction-diffusion model to estimate the rate of transport for CO_2 within the particles. Previous work at Notre Dame and LLNL provides the necessary ionic liquid reactivity and diffusivity and the permeability of the polymer shell. We found that the primary mass transfer resistance is in the core where the CO_2 diffuses, and then reacts with the ionic liquid. The following figure (**Figure 28**) shows the concentration front of reacted (complexed) CO_2-IL as it propagates into a 400 μm diameter capsule over 500 s.

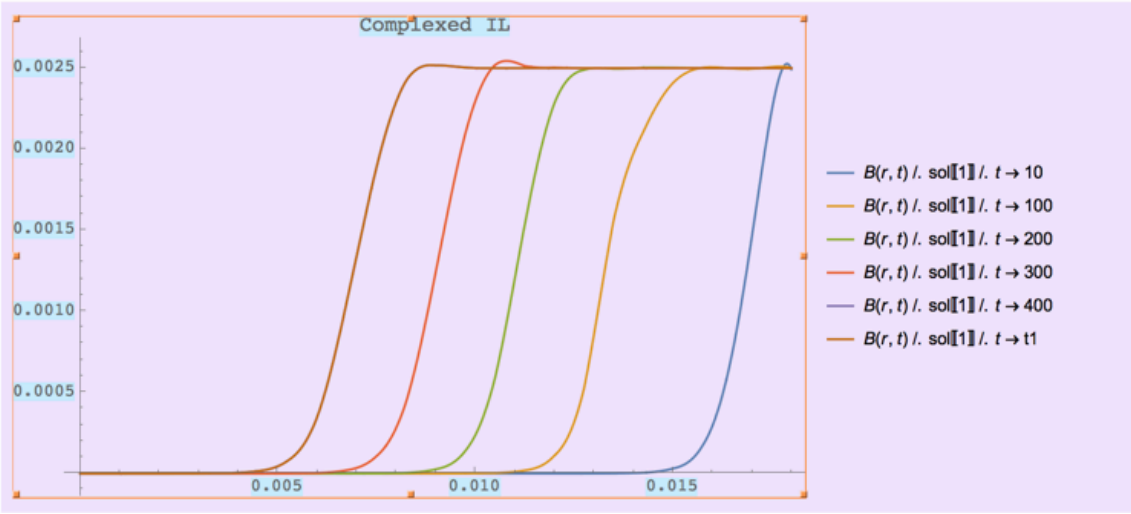

Figure 28: Concentration front of reacted (complexed) CO_2-IL as it propagates into a 400 μm diameter capsule over 500 seconds.

In a cyclic process there would be some optimal degree of saturation of the capsules. However we can see that this time scale is likely 100's of seconds.

Figure 29 shows the calculated rates of diffusion of CO_2 over the expected range of candidate shell material permeabilities.

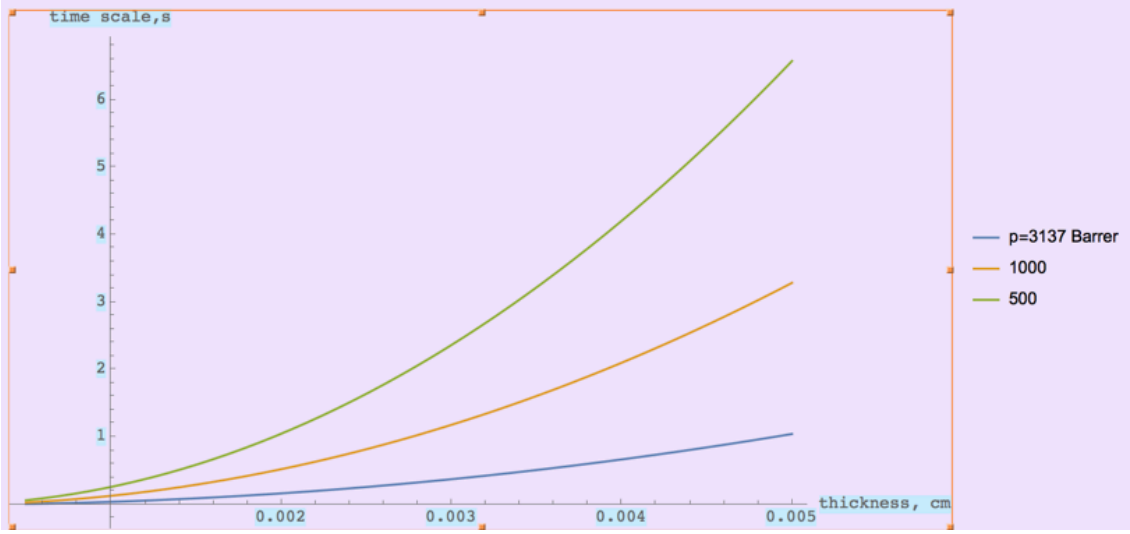

Figure 29: Calculated rates of diffusion of CO_2 over the expected range of candidate shell material permeabilities

Even for the 50 μm thick, low permeability (500 Barrer) material, the time scale is only about 6 s which is much less than the 100's of seconds that would be required to saturate the IL in the core.

From these calculations, we can determine that even for a quantity a small as 10 grams of 400 μm capsules, which would contain about 0.02 moles of IL, the surface area and absorbance rates are such that we could absorb ~7 x 10^{-5} moles CO_2/s. For gas flows in the range of minimum fluidization, we could remove about ½ of the CO_2 (at say 15 mole %) in a single pass through the bed. This is well within the range of the CO_2 analyzers. There would hence be no need to cause multiple passes of the gas through the bed.

The overall schematic of the flow system is shown below (**Figure 30**). We have completed the design and equipment selection. Construction was done in such a way as to allow completion of Subtask 4.2 (above) along the way.

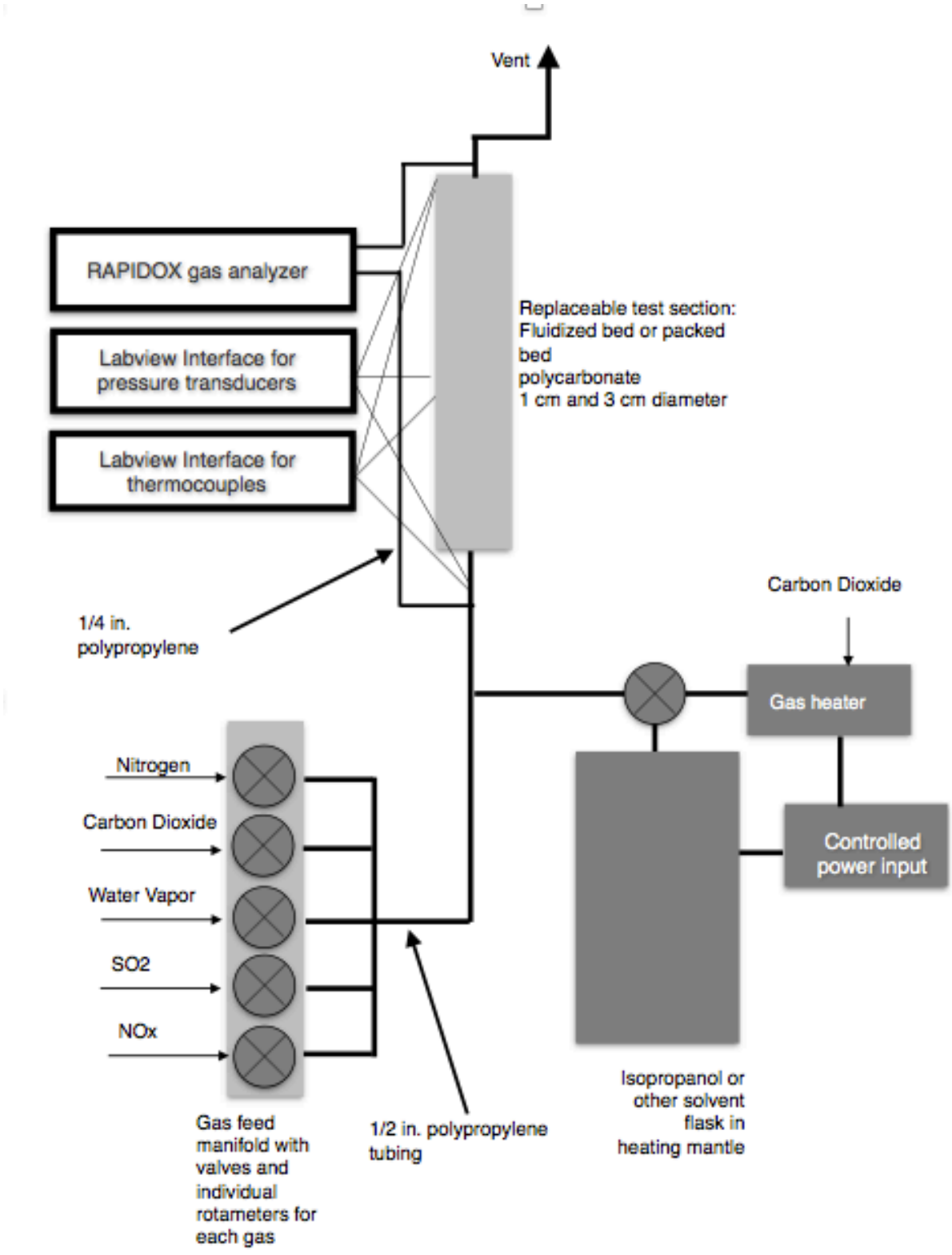

Figure 30: Experimental system schematic

A recent photo of the construction progress is shown in **Figure 31**.

Figure 31: Picture of skid mounted experimental rig.

This frame is in a walk-in hood that allows the gas cylinders to remain outside of the hood.

Subtask 6.2 - Design of packed bed absorber/desorber

Much of the discussion of mass transfer inside the particles and ranges of flow rates given above applies to this task. Further, it is certain that running this process in a fluidized bed is preferred to a packed bed. Since the mechanical testing has confirmed the robustness of the capsules, we don't expect that it will ultimately be necessary to design a packed bed system for absorption. However, we completed this task. The flow rates and size are such that a packed bed column will simply replace a fluidized bed in our apparatus. We will place a screen barrier above the packed region to keep the capsules in place.

For the 300 μm spheres, the pressure drop is about 0.2 atm/m if the superficial velocity is 10 cm/s. If we use 10 g of capsules in a 1 cm diameter column, the total height of packing will be about 20 cm. The 10 g of capsules will contain about 0.02 mol IL. As noted above these can be saturated in about 300 s. Thus we can absorb 1.4×10^{-4} mole/s. Since we can operate a packed bed at the same flow rates as the fluidized bed, with almost the same mass transfer performance because the internal capsule resistance dominates, there should be no problem in measuring the change in CO_2 concentration across the bed.

Subtask 6.3 - Design of condensable vapor regeneration system

For a column diameter of 1 cm, only 3-10 cm^3/s of vapor flow is needed to fluidize the capsules. Basing calculations on isopropanol as a condensable vapor that could be used to heat the particles and carry away the CO_2 (and still be condensed to produce CO_2 at high purity), a 500 ml boiling flask with 500 W heating mantle controlled with Variac could give >500 s of vapor at up to 300 cm^3/s. This would be plenty of flow and capacity to regenerate the capsules.

It is worthwhile to note however, that it is likely that an industrial process would be more cost effective if an external component were not added. That is, if instead of a condensable vapor, we just used sufficiently hot CO_2. So we will be sure to do experiments that use hot CO_2 for regeneration.

Subtask 6.4 - Selection and ordering of all system components

With the design in hand, we began ordering components and assembling the system beginning in August. At the present time, construction is more than 50% completed as shown in **Figure 31**.

CONCLUSIONS

Nineteen IL and PCIL candidates have been synthesized and tested, which include measurements of melting points, glass transition temperatures, decomposition temperatures, enthalpies of fusion, viscosities, densities and CO_2 uptake. One of each has

been selected for encapsulation and testing. Several polymer encapsulation formulations have been developed and tested. Chemical compatibility problems with one of the formulations, SiTRIS, led to reduced CO_2 capacity. However, the thiolene cured silicone capsules do not react with the IL and PCIL, and the encapsulated NDIL0309 has CO_2 capacity comparable to the bulk PCIL. Rate-based models have been developed for both fluidized and packed beds of the encapsulated IL or PCIL particles and the laboratory scale unit has been designed, the equipment ordered and the construction is well underway.

REFERENCES

1. Hong, B.; Simoni, L. D.; Bennett, J. E.; Brennecke, J. F.; and Stadtherr, M. A., "Simultaneous Process and Material Design for Aprotic N-Heterocyclic Anion Ionic Liquids in Post-Combustion CO_2 Capture," submitted to Ind. Eng. Chem. Res., 2016.
2. Seo, S.; Quiroz-Guzman, M.; DeSilva, M. A.; Lee, T. B.; Huang, Y.; Goodrich, B. F.; Schneider, W. F.; and Brennecke, J. F., "Chemically Tunable Ionic Liquids with Aprotic Heterocyclic Anions (AHAs) for CO_2 Capture," J. Phys. Chem. B, 2014, 118, 5740-5751. DOI 10.1021/jp502279w.
3. Fillion, J. H.; Xia, H.; DeSilva, M. A.; Quiroz-Guzman M.; and Brennecke, J. F., "Phase Transitions, Decomposition Temperatures, Viscosities and Densities of Phosphonium, Ammonium and Imidazolium Ionic Liquids with Aprotic Heterocyclic Anions," J. Chem. Eng. Data, 2016, 61(8), 2897-2914.
4. Seo, S.; DeSilva, M. A.; Xia H.; and Brennecke, J. F., "Effect of Cation on Physical Properties and CO_2 Solubility for Phosphonium-Based Ionic Liquids with 2-Cyanopyrrolide Anions," J. Phys. Chem. B, 2015, 119, 11807-11814.
5. Seo, S.; Simoni, L. D.; Ma, M.; DeSilva, M. A.; Huang, Y.; Stadtherr, M. A.; and Brennecke, J. F., "Phase-Change Ionic Liquids for Postcombustion CO_2 Capture," Energy & Fuels, 2014, 28(9), 5968-5977.
6. Thompson, R. L.; Shi, W.; Albenze, E.; Kusuma, V. A.; Hopkinson, D.; Damodaran, K.; Lee, A. S.; Kitchin, J. R.; Luebke, D. R.; and Nulwala, H., "Probing the effect of electron donation on CO_2 absorbing 1,2,3-triazolide ionic liquids," RSC Advances, 2014, 4(25), 12748-12755.
7. Vericella, J. J.; Baker, S. E.; Stolaroff, J. K.; Duoss, E. B.; Hardin IV, J. O.; Lewicki, J.; Glogowski, E.; Floyd, W. C.; Valdez, C. A.; Smith, W. L.; Satcher, J. H. Jr.; Bourcier, W. L.; Spadaccini, C. M.; Lewis, J. A.; and Aines, R. D., "Encapsulated liquid sorbents for carbon dioxide capture," Nat. Commun., 2015, 6, 1–7.
8. Powell, C. E. and Qiao, G. G., "Polymeric CO_2/N_2 gas separation membranes for the capture of carbon dioxide from power plant flue gases," J. Membr. Sci. 2006, 279, 1–49.
9. Haslbeck, J. L.; Kuehn, N. J.; Lewis, E. G.; Pinkerton, L. L.; Simpson, J.; Turner, M. J.; Varghese, E.; Woods, M. C., "Cost and Performance Baseline for Fossil Energy Plants, Volume 1: Bituminous Coal and Natural Gas to Electricity, Revision 2a," Report DOE/NETL-2010/1397, National Energy Technology Laboratory, 2013.
10. Fischer, K.; Beitler, C.; Rueter, C.: Searcy, K.; Rochelle, G.; and Jassim, M., "Integrating MEA regeneration with CO_2 compression and peaking to reduce capture

costs," Trimeric Corporation. 2005. (http://www.trimeric.com/Report060905.pdf).
11. Yang, W. C. and Hoffman, J., "Exploratory design study on reactor configurations for carbon dioxide capture from conventional power plants employing regenerable solid sorbents," Ind. Eng. Chem. Res., 2008, 48(1): 341-351.
12. Myers, D.; Fisher, K.; Beitler, C.; and Sexton, A., "Systems Analysis of Ionic Liquids Sorbents for CO_2 Capture," Ninth Annual Conference on Carbon Capture and Sequestration, Pittsburgh, PA, May 10-13, 2010.

ACKNOWLEDGEMENT

This material is based upon work supported by the Department of Energy under Award Number DE-FE0026465.